National Library of Canada   **Bibliothèque nationale du Canada**

Canadian Theses Division   Division des thèses canadiennes

Ottawa, Canada
K1A 0N4

49116

PERMISSION TO MICROFILM — AUTORISATION DE MICROFILMER

- Please print or type — Écrire en lettres moulées ou dactylographier

Full Name of Author — Nom complet de l'auteur

PETER   MALCOLM   STEFFLER

Date of Birth — Date de naissance	Country of Birth — Lieu de naissance
November 12, 1956	CANADA

Permanent Address — Résidence fixe

10706   67 AVE.   EDMONTON   ALBERTA   T6H 1Z9

Title of Thesis — Titre de la thèse

DEFLECTION   OF   JETS   BY   WEAK   CROSSFLOWS

University — Université

UNIVERSITY OF ALBERTA

Degree for which thesis was presented — Grade pour lequel cette thèse fut présentée

MASTER   OF   SCIENCE

Year this degree conferred — Année d'obtention de ce grade	Name of Supervisor — Nom du directeur de thèse
1980	N. RAJARATNAM

Date	Signature
Oct. 15 / 1980	

NL-91 (4/77)

NOTICE

AVIS

The quality of this microfiche is heavily dependent upon the quality of the original thesis submitted for microfilming. Every effort has been made to ensure the highest quality of reproduction possible.

If pages are missing, contact the university which granted the degree.

Some pages may have indistinct print especially if the original pages were typed with a poor typewriter ribbon or if the university sent us a poor photocopy.

Previously copyrighted materials (journal articles, published tests, etc.) are not filmed.

Reproduction in full or in part of this film is governed by the Canadian Copyright Act, R.S.C. 1970, c. C-30. Please read the authorization forms which accompany this thesis.

La qualité de cette microfiche dépend grandement de la qualité de la thèse soumise au microfilmage. Nous avons tout fait pour assurer une qualité supérieure de reproduction.

S'il manque des pages, veuillez communiquer avec l'université qui a conféré le grade.

La qualité d'impression de certaines pages peut laisser à désirer, surtout si les pages originales ont été dactylographiées à l'aide d'un ruban usé ou si l'université nous a fait parvenir une photocopie de mauvaise qualité.

Les documents qui font déjà l'objet d'un droit d'auteur (articles de revue, examens publiés, etc.) ne sont pas microfilmés.

La reproduction, même partielle, de ce microfilm est soumise à la Loi canadienne sur le droit d'auteur, SRC 1970, c. C-30. Veuillez prendre connaissance des formules d'autorisation qui accompagnent cette thèse.

THIS DISSERTATION HAS BEEN MICROFILMED EXACTLY AS RECEIVED

LA THÈSE A ÉTÉ MICROFILMÉE TELLE QUE NOUS L'AVONS REÇUE

THE UNIVERSITY OF ALBERTA

DEFLECTION OF JETS BY WEAK CROSSFLOWS

by

PETER M. STEFFLER

A THESIS

SUBMITTED TO THE FACULTY OF GRADUATE STUDIES AND RESEARCH

IN PARTIAL FULFILMENT OF THE REQUIREMENTS FOR THE DEGREE

OF MASTER OF SCIENCE

DEPARTMENT OF CIVIL ENGINEERING

EDMONTON, ALBERTA

FALL 1980

THE UNIVERSITY OF ALBERTA

FACULTY OF GRADUATE STUDIES AND RESEARCH

The undersigned certify that they have read, and
recommend to the Faculty of Graduate Studies and Research,
for acceptance, a thesis entitled DEFLECTION OF JETS BY WEAK
CROSSFLOWS submitted by PETER M. STEFFLER in partial
fulfilment of the requirements for the degree of MASTER OF
SCIENCE.

....

Supervisor

....

....

Date...29 Sept '80.........

Abstract

A common problem in the field of enviromental fluid mechanics is the disposal of an effluent into a moving ambient fluid. The prediction of concentration contours is important in these cases to be able to evaluate the impact of the effluent. In cases where the effluent discharge velocity is large compared to the ambient velocity the problem may be modeled as a turbulent jet. The purpose of this study is to investigate the effect of a weak crossflow on such a jet.

The study was done by first performing an experimental investigation. The situation modeled in the experiments was that of a jet discharged on the bed of a curved channel. The experimenal study provided a physical appreciation and the means for theoretical approximations. Essentially, it was found that the jet behaviour was not significantly altered by the presence of the crossflow except that the jet was deflected from a straight line path.

To theoretically predict the deflection of the jet a number of simpler problems were considered as well as the curved channel problem. The procedure, however, was the same. A moment of momentum equation was derived and simplified and was found in all cases to predict the deflection given the variation of the other scales and without the need of additional empirical constants.

The theoretical predictions were compared with various observations and were found to be valid for the initial portion of the deflected jet up to a limit which varies with the relative magnitudes of the initial jet velocity, ambient longitudinal velocity, and ambient lateral velocity.

Acknowledgements

The author would like to express his sincere gratitude to Dr. N. Rajaratnam for his sustained encouragement and guidance throughout the course of this study.

The technical assistance provided by Messrs. S. Lovell, D. McGowan, and R. Gitzel is gratefully acknowledged. Financial support for the author was provided by a Postgraduate Scholarship from the Natural Science and Engineering Research Council and supplemented by the Department of Civil Engineering. The study was also supported by the Natural Science and Engineering Research Council through a grant to Dr. N. Rajaratnam. These are gratefully acknowledged.

Finally, the author is immeasurably indebted to his wife, Gail, for her encouragement and understanding as well as her able assistance throughout the study.

Table of Contents

List of Figures

List of Tables and Photographic Plates

List of Symbols

b	transverse length scale
b_0	initial half-width of jet
b	lateral length scale
b	vertical length scale
d	lateral deflection of jet
f_i	lateral profile functions
g_j	vertical profile functions
h	depth of flow
m	empirical constant
n	empirical constant
p	pressure
r_c	initial radius of circular jet
u	longitudinal velocity
u_m	maximum jet velocity at a section
v	lateral velocity
w	vertical velocity
x	longitudinal coordinate
y	lateral coordinate
z	vertical coordinate
C	empirical constant
F_i	integral constants
I_i	integral constants
K_i	empirical constants
R	radius of curvature
U	ambient longitudinal velocity
U_0	initial jet velocity

V	ambient lateral velocity
V_0	initial ambient lateral velocity
α	initial jet to longitudinal ambient velocity ratio
β	ambient lateral to longitudinal velocity ratio
δ	nondimensional deflection
ζ	nondimensional vertical coordinate
η	nondimensional lateral coordinate
θ	momentum thickness
υ	kinematic viscosity
ξ	nondimensional longitudinal coordinate
ρ	fluid density
τ_{ij}	fluid shear stresses
Ξ	function of longitudinal coordinate
Ω	gravitational potential

0.1 Introduction

0.1.1 Purpose

The effect of lateral currents on turbulent jets and plumes is a complicated three dimensional problem in the field of enviromental fluid mechanics. Much work has been done on this problem, mostly of an experimental nature, but general results are few. It is the objective of the present study to investigate the effect of weak lateral currents on turbulent jets. A specific practical problem to be considered is a circular turbulent wall jet discharging into a curved co-flowing stream.

0.1.2 Practical Significance

Accurate prediction of the enviromental effects of industrial and domestic waste disposal is becoming ever more important in the world today. The first step in predicting these effects is normally to calculate the pollutant concentration field. The tools available for this calculation are jet theory, diffusion theory, and dispersion theory. Each has it's own range of applicability and limitations. In some problems all three approaches may be required to cover the appropriate range of interest. The present study is concerned with the problems in the domain of jet theory.

Jet theory is most useful near the pollutant outlet, where concentrations are highest. The excess momentum of the jet causes entrainment of the ambient fluid resulting in rapid mixing and dilution. Bouyancy effects may or may not be important. The ambient fluid body may be a stream, a river, lakes of various sizes, the ocean, or the atmosphere. Rarely, however, is the ambient fluid at rest. Thus, to accurately predict the pollutant concentration field, the effect of the ambient motion on the jet and pollutant mixing must be known. Essentially, the calculation of pollutant mixing by a jet is accomplished by calculation of the velocity field. Using Reynold's hypothesis modified to fit the experimental data, the concentration field may be calculated from the velocity field through the use of a pollutant conservation equation.

The present study is concerned with the discharge of jets into a moving ambient fluid with a small lateral component (relative to the jet). Some examples of practical situations are: a jet discharging into a stream at a small angle to the flow, a jet discharging into a curved channel flow, a bouyant plume discharged into an ocean current, and a heated surface discharge onto a lake with circulation.

Although the results of this study may be applied to any of these cases, the emphasis will be on the case of a discharge into a curved channel. As most natural channels

are curved to some extent, the resulting behavior of a
pollutant discharge is of considerable practical importance.

0.1.3 Sketch of Proposed Work

The effect of lateral currents on turbulent jets was
investigated by the following procedure. First, an
experimental procedure was devised to obtain qualitative
information useful in problem simplification. The
arrangement used was that of a circular wall jet injected
longitudinally into a curved channel flow. This setup
simulated to some extent the practical situation of a
pollutant diffuser in a natural channel. Velocity profiles,
both vertical and lateral, were taken at a number of
downstream locations for a range of initial velocity ratios.
The position of the jet in the channel cross-section was
also varied.

The results of the experiments were analysed with
respect to similarity of profiles and downstream scale
variation. These results were then compared to the results
of a similar study in a straight channel. Qualitatively, the
effect of the crossflow was observed and the important
parameters noted.

Using the simplifications afforded by the experimental
results, a theoretical analysis was made of a similar but
more basic situation. The essential assumption justified by

the experimental results was that the cross-sectional profiles of the downstream component of excess velocity remained similar. With this assumption, integral momentum, energy, and moment of momentum equations were derived. These equations provided the means to calculate the the variation of the width scale, velocity scale, and deflection of the jet in the downstream direction. The latter parameter and terms involving the crossflow were found to occur only in the moment of momentum equation thus allowing the first two equations to be solved separately and the results substituted into the third to explicitly calculate the deflection.

Various simplified problems were studied and the results compared to experimental data where available. Finally, the theory was applied to the experimental work and the results compared.

0.2 Review of Existing Work

0.2.1 Jets in Crossflow

In recent years the subject of jets in crossflows has recieved considerable attention from various researchers. The earlier studies were primarily of an experimental nature including descriptive observation and empirical predictive formulae. Notable studies include Pratte and Baines (1967) Keffer and Baines (1963) and Gordier (1959).

Based on these observations three separate regions of the deflected jet may be distinguished. The first, the near field, is characterized by high jet velocity to crossflow velocity ratio, and small deflections. The second region, the curvilinear region, is characterized by large ambient fluid entrainment, rapid jet velocity decay, and large deflection. The characteristic 'kidney' shaped velocity contours develop in this region. The third region, the vortex region, is characterized by a pair of counterrotating vortices generated in the wake of the deflecting jet. By this time the jet axis is nearly parallel to the ambient fluid direction. In any analysis the special features of each region must be maintained in consideration.

With reference to the present study, attention is focused only on the initial near field region. Even then, only the special situation wherein this region is much longer than the potential core length is considered.

The early studies provided empirical expressions for the deflected jet axis usually in the form of a power law ie:

$$\frac{d}{b_0} = C \, \beta^n \left(\frac{x}{b_0} \right)^m \tag{1}$$

where x is longitudinal distance, d is deflection , β is the

initial jet to crossflow velocity ratio, b_0 is nozzle radius, and C, n, and m are empirical constants. Often, the expression was inverted to give the penetration as a function of downstream distance. In some cases the exponent and constant were evaluated separåtly for the different regions but usually one formula was fitted to the entire jet. A review of these formulae appears in Rajaratnam (1976).

Early analytical approaches to this problem, such as Abramovich (1963) and Crowe and Reisbieter (1967) were based on the principle that the deflection of the jet is caused by a pressure differential analogous to the drag force on a cylinder. It was found however, that this mechanism could not account for the deflection unless unrealistically high values of the drag coefficent were chosen.

A later study, Platten and Keffer (1968), introduced the mechanism of entrainment as the cause of jet deflection. Essentially, the jet obtains momentum in the lateral direction by entrainment of the ambient fluid. This entrainment was found to be larger than for free jets but the form of the entrainment relation and coefficents proved difficult to evaluate.

The most recent analytical studies by Chan, Lin, and Kennedy (1976), Wright (1977) and Makibata and Miyai (1979)

all recognize the three separate regions and use both drag
and entrainment concepts to calculate the deflection and
other parameters. The Chan, Lin, and Kennedy study, in
particular, uses integrated equations of motion and
similarity relations in the calculation. In regard to the
near field region, however, the deflection is taken simply
as a consequence of lateral convection and the equation for
the deflection is:

$$\frac{dd}{dx} = \frac{V}{u_m} \tag{2}$$

Generally, these studies were primarily concerned with
jets discharging perpendicular to the ambient fluid
direction although some observations on oblique jets were
also presented. Bouyancy effects were also investigated,
particularly by Wright (1977). No study, however, included
wall effects.

0.2.2 Turbulent Jets

The mechanics of turbulent jets is a well studied
problem and all the essential information used herein may be
easily obtained in Rajaratnam (1976). Of particular interest
is the problem of compound jets. The results of an analysis
by Pande and Rajaratnam (1979) are used in simplified form
in the present study. Circular compound wall jets were

studied experimentally by Stalker (1979).

0.2.3 Curved Channel Flow

Since Thomson (1876) noted the presence of a spiral current in the flow around bends of streams, much investigation has been made into the problem. The most notable studies were Einstien and Harder (1956), Rozovski (1957), Yen(1965), and Engelund (1974). Due to the complexity of the problem, these investigators were concerned mainly with the special case of developed or axisymmetric flow. They did however, obtain useful information about the magnitude and shape of the lateral velocity distribution. In particular, the approximate relation due to Engelund (1974):

$$\frac{V}{U} \simeq 7 \frac{h}{R} \tag{3}$$

where h is the depth of flow, R is the radius of curvature, U is mean downstream velocity, and V is lateral velocity gives an estimate of the magnitude of the crossflow near the bed. Over the depth of the jet the average velocity ratio is given by changing the constant to about three.

1. EXPERIMENTAL INVESTIGATION

1.1 Experiments

1.1.1 Apparatus and Equipment

1.1.1.1 Flume

The flume used was curved in an 'S' shape with two consecutive 180 degree bends of 9.0 feet centerline radius. The test section was located at 90 degrees into the second bend. A plan of the flume is shown in figure (1) and a view of the test location is shown in plate (1). The flume was located at the Ellerslie River Engineering research station of the University of Alberta.

The flume is equiped with it's own sump and pump and has an adjustable tailgate to regulate flow depth. The table slope of the flume is adjustable but was mantained level for the experiments. The bed was smooth aluminum and was marked with a curvilinear grid for qualitative reference.

1.1.1.2 Traverse

The traverse used provided electrically powered motion in the lateral and vertical directions but required manual adjustment in the longitudinal direction. The lateral position was measured electronicly by means of a potentiometer to the nearest one hundredth of a foot while the vertical position was measured visually using a staff gauge with a vernier to the nearest one thousandth of a
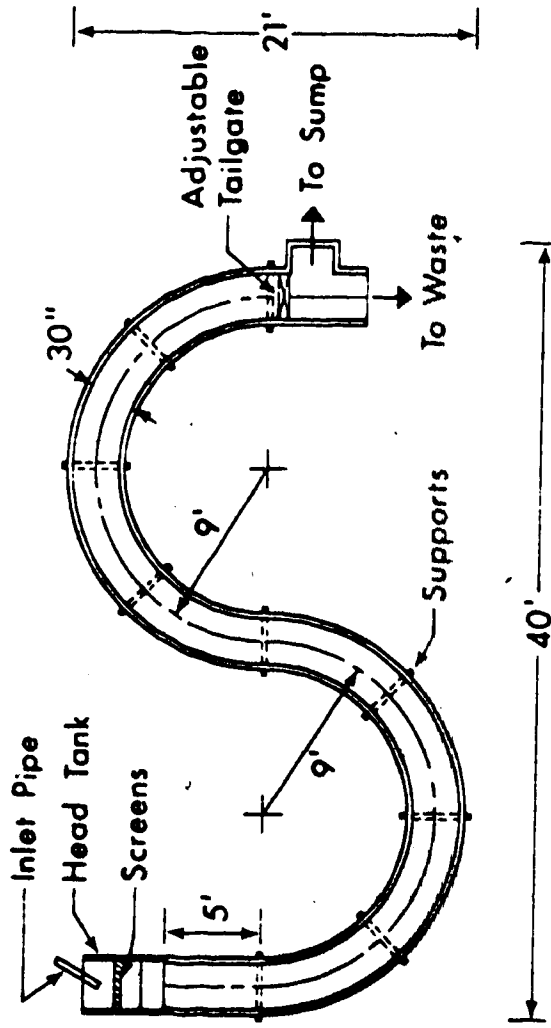
Figure 1 - Plan of Curved Flume
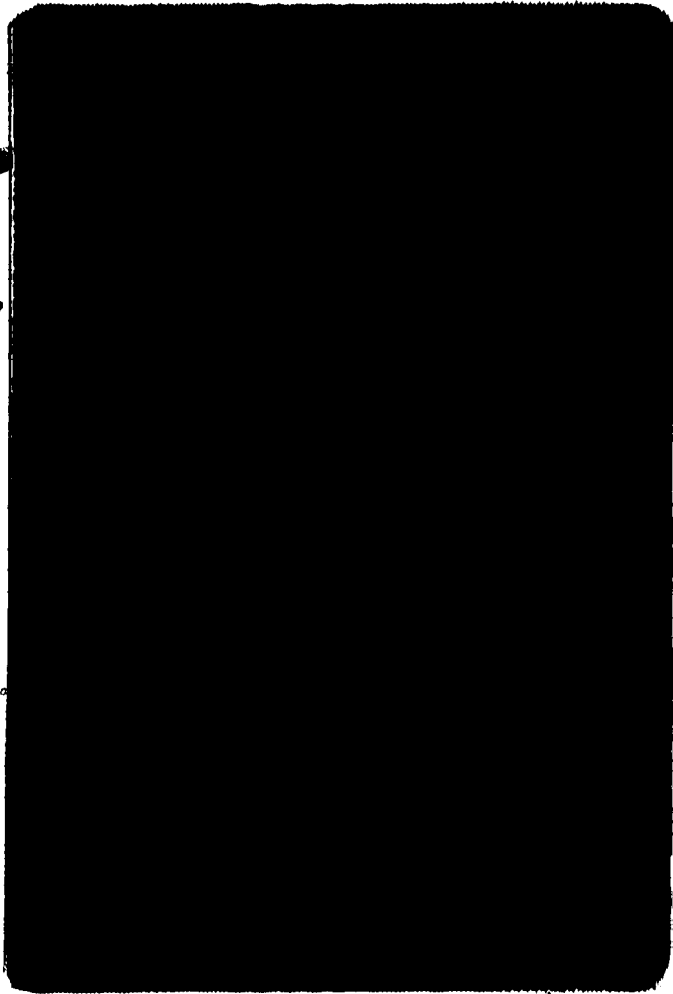
Plate 1 - Test Location

foot. The downstream locations were set at 0.2 foot intervals along lines tangent to the curve at the jet location. Plate (2) shows the traverse.

1.1.1.3 Jet Arrangement

The jet arrangement involved a constant head device, large diameter tubing, and a nozzle. The constant head device was mounted on an adjustable stand and fed by a hose directly from the city water supply. The tubing was 3/4 inch inside diameter plastic 'Tygon Tubing' and was about five feet in length. The nozzle was a steamlined tube bent at a 90 degree angle at the bottom to the exit. It was introduced into the flow through the water surface to the bed. This resulted in some disturbance to the flow but was necessary because of the requirement that the location of the jet be changed easily. The inside diameter of the tube portion was 3/8 inch and the outlet diameter was 1/4 inch.

The elevation of the water in the head tank was not measured because it was found that the losses in the tubing and nozzle were very significant and therefore the only reliable measurement of initial velocity was an actual velocity reading in the potential core of the jet.

Two flaws of this setup became apparent during and after the course of experiments. The first was that the jet flow was at city water temperature while the channel flow

Plate 2 - Traverse for Velocity Measurements

tended to be at room temperature, resulting in possible bouyancy effects. The second problem was that there was no provision to accurately align the jet with the coordinate system. As a consequence the measured deflections proved difficult to correlate.

1.1.1.4 Measurement System

Velocity measurements were made by means of a standard Prandtl tube of 1/8 inch outside diameter. The pressure difference was measured with a sloping manometer set at 0, 60, and 75 degrees from the vertical depending on the magnitude of the velocity. At the flatest setting, pressure differentials could be measured to the nearest one thousandth of a foot of water.

Water surface slope was measured by means of two static head screwdriver type probes placed at 45 degrees upstream and downstream of the jet location. The depth at these locations was indicated on the same sloping manometer as the velocity readings.

A yaw probe was also considered for use but the additional information about the lateral velocities was found to be unreliable due to the width of the probe compared to the lateral velocity gradient.

1.1.2 Procedure

1.1.2.1 Preliminary Runs

A series of preliminary runs were performed in order to qualitatively examine the problem. These runs used the equipment described above but no velocity measurements were made other than to obtain an initial velocity ratio. Instead, the injected water was dyed and the dispersion of the jet was visually studied. A typical plot of a visually time averaged jet profile is shown in figure (2). A photograph of the dyed jet is shown in plate (3). Note that the plot is referenced to the arc of the curve determined by the location of the jet. Various parameters such as velocity ratio, channel Reynolds and Froude numbers, and lateral position of the jet were varied. The parameters selected for further study were the velocity ratio and jet position.

1.1.2.2 Actual Runs

After completion of the preliminary runs a series of six more detailed runs were performed. Table (1) indicates the appropriate parameters for each experiment. Figure (3) is the definition sketch for this data. The object of these runs was to obtain qualitative and quantitative information about the velocity distribution of the jet.

Each experiment involved taking a lateral and vertical velocity profile at three or four downstream stations. The only component of velocity measured was the 'u' component;
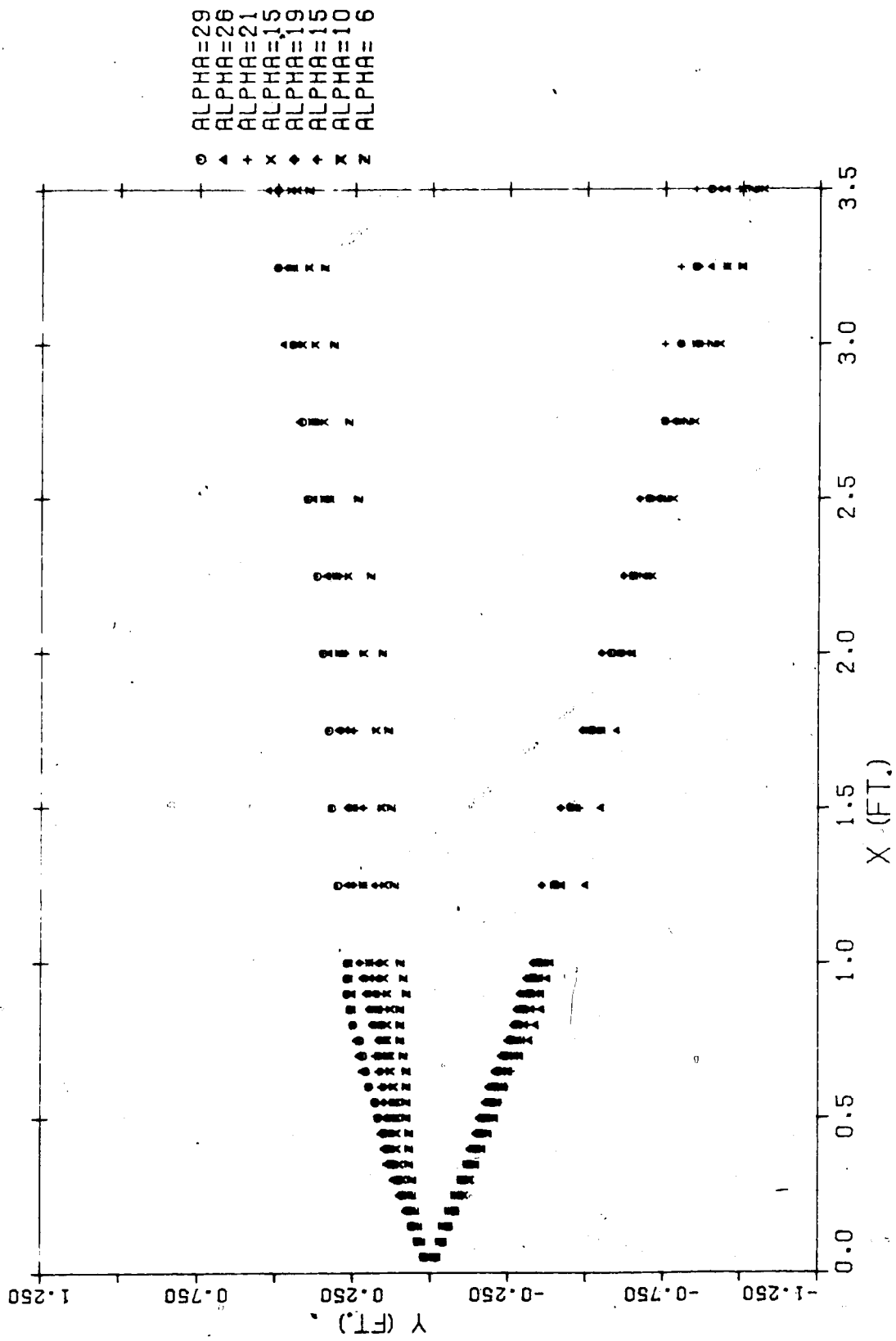
Figure 2 - Plot of the Boundaries of Dyed Jet (Plan View)
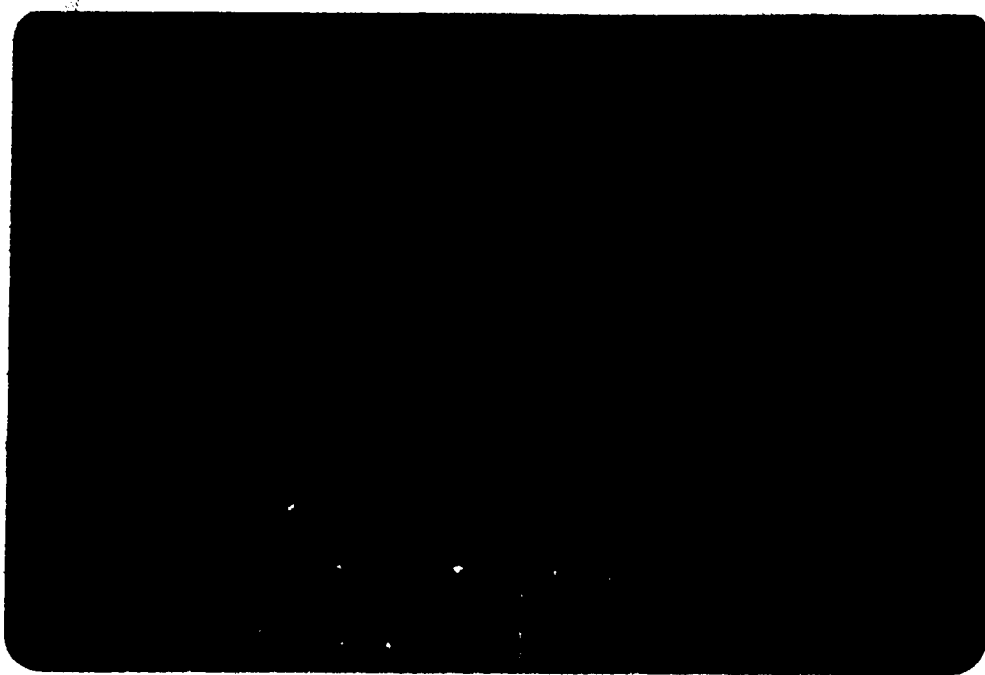
Plate 3 - Plan View of Dyed Jet

RUN NO.	U_o FT/S	U FT/S	α	θ FT.	R/θ	R_e	POS.
1	4.35	1.0	4.35	.0398	226.1	5440	M
2	7.24	.80	9.05	.0889	101.2	9050	M
3	7.39	.80	9.24	.0909	110.0	9240	O
4	7.47	.80	9.34	.0919	87.1	9340	I
5	3.25	.80	4.06	.0367	272.5	4060	O
6	9.30	.70	13.29	.1331	75.1	11630	O

Table 1 - Significant Details of the Experiments

18
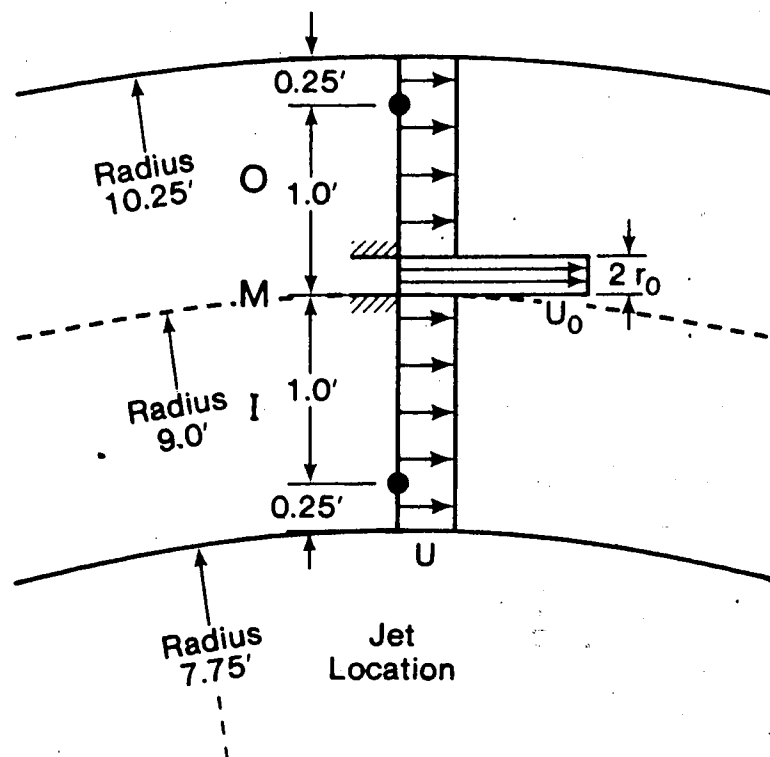
Figure 3. Experiment Definition Sketch.

that is, the component parallel to the initial jet axis. The
lateral profile was taken first with the Prandtl tube
slightly above the flume bed. The results of the lateral
profile were plotted as they were taken and the position of
maximum velocity noted. About ten points were found to be
sufficent to describe the lateral profile.

The vertical profile was taken at the location of
maximum velocity as indicated by the lateral profile. The
first reading was taken with the tube resting on the bed and
subsequent readings were taken at spacings upward to allow
the profile to be adequately defined with approxiametly ten
points. The elevation of the lateral profile was checked to
insure that it was reasonably close to the elevation of
maximum velocity.

To insure that air bubbles did not interfere with the
readings, the system was flushed before each profile.
Readings were then taken in order of decreasing velocity to
prevent the air rich ambient water from entering the system.
For the lateral profiles this involved alternating the pitot
tube from side to side of the centerline and further away.

Figures (4)-(15) show the vertical and lateral velocity
profiles for all sections of runs one to six.

Figure 4 - Run 1 Lateral Profiles of Longitudinal Velocity

Figure 5 - Run 1 Vertical Profiles of Longitudinal Velocity

Figure 6 - Run 2 Lateral Profiles of Longitudinal Velocity
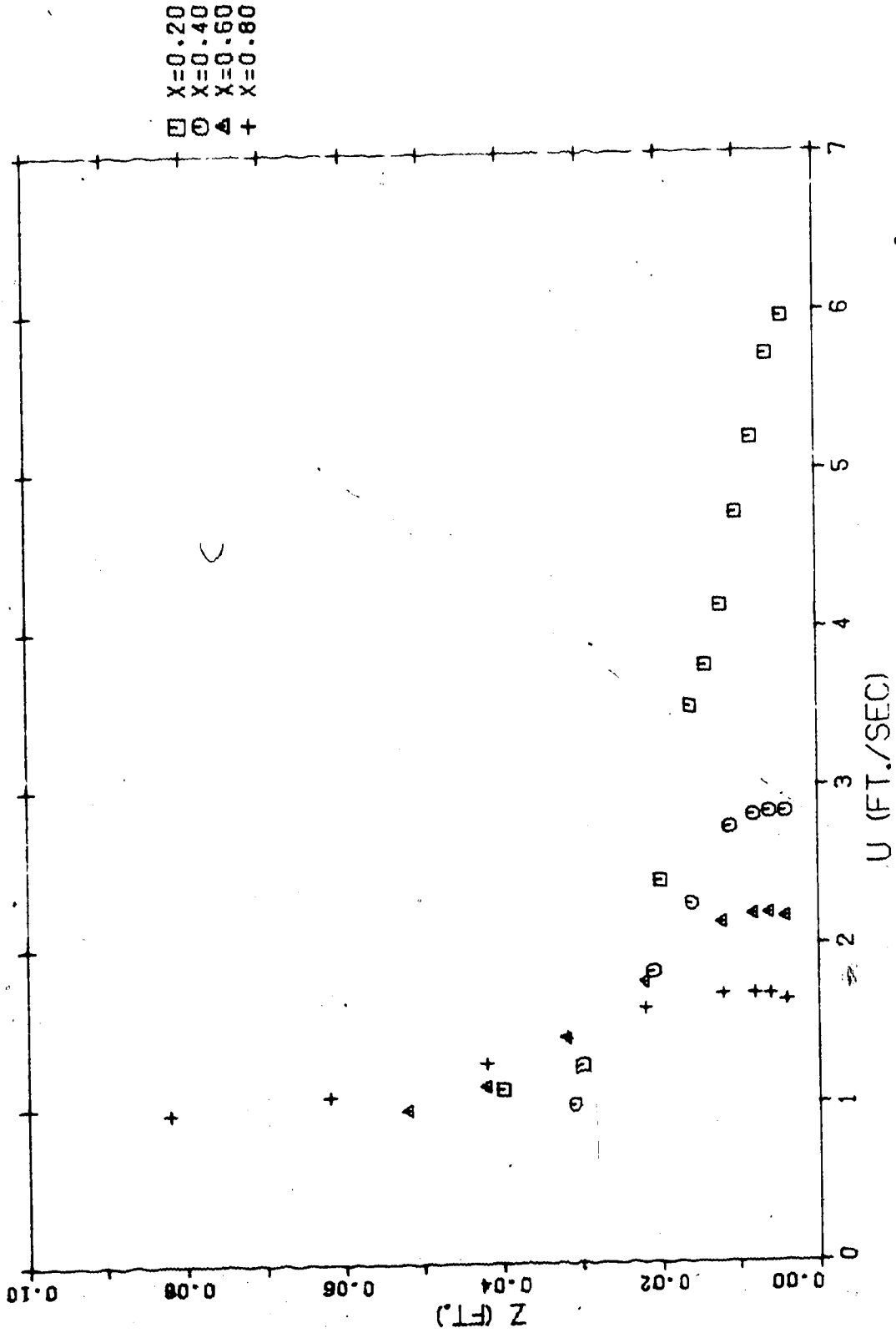
Figure 7 - Run 2 Vertical Profiles of Longitudinal Velocity
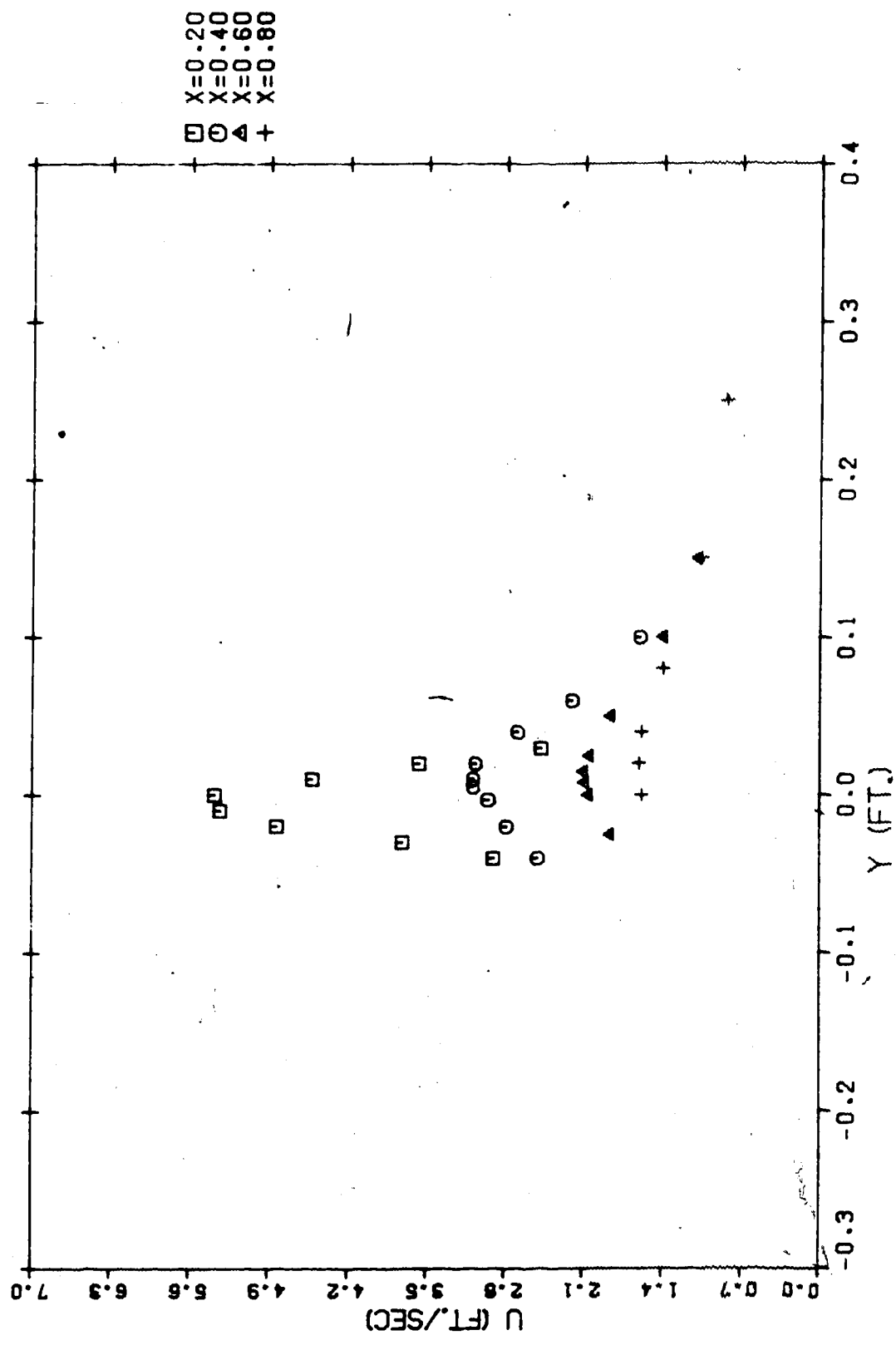
Figure 8 - Run 3 Lateral Profiles of Longitudinal Velocity
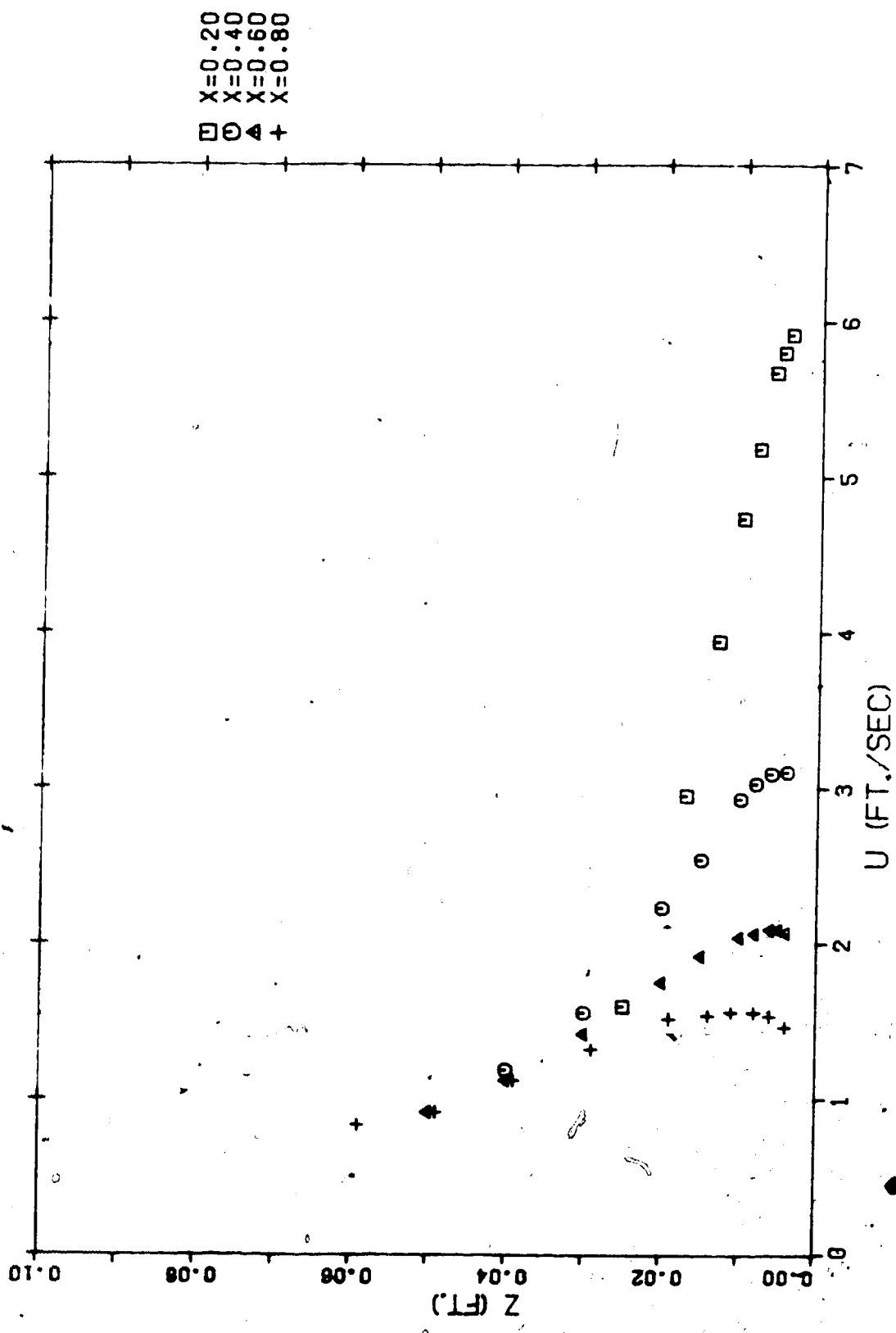
Figure 9 - Run 3 Vertical Profiles of Longitudinal Velocity
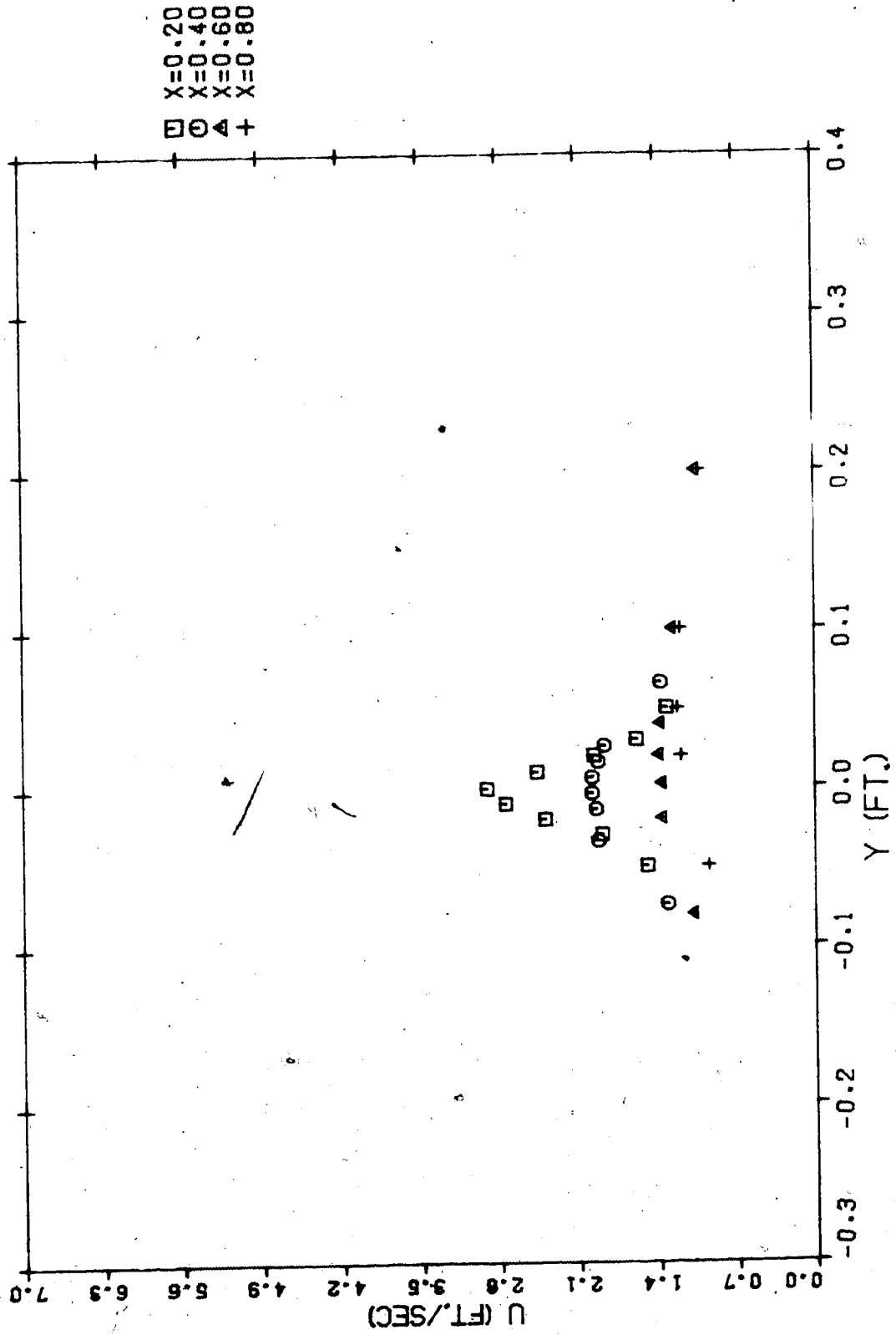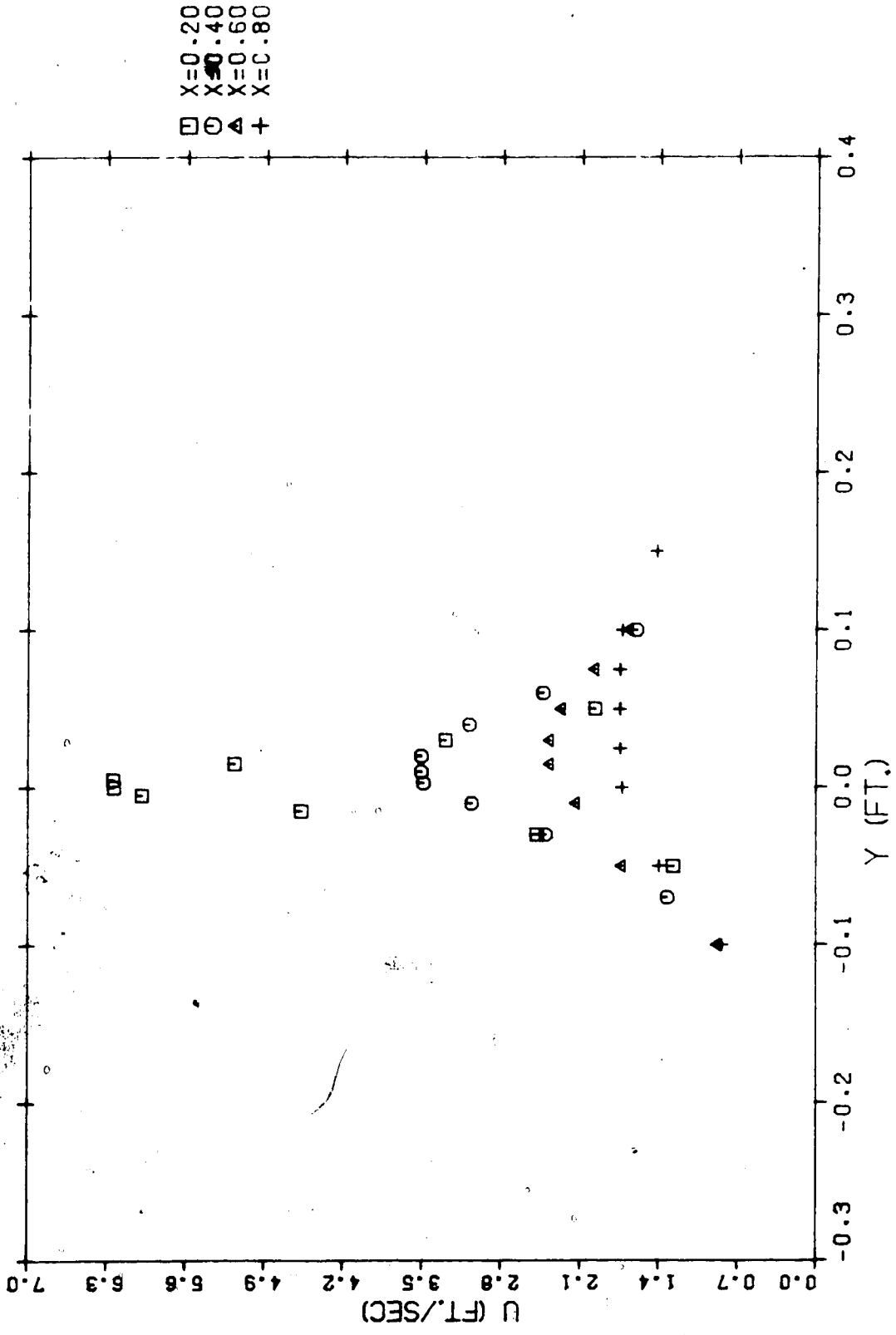
Figure 10 - Run 4 Lateral Profiles of Longitudinal Velocity
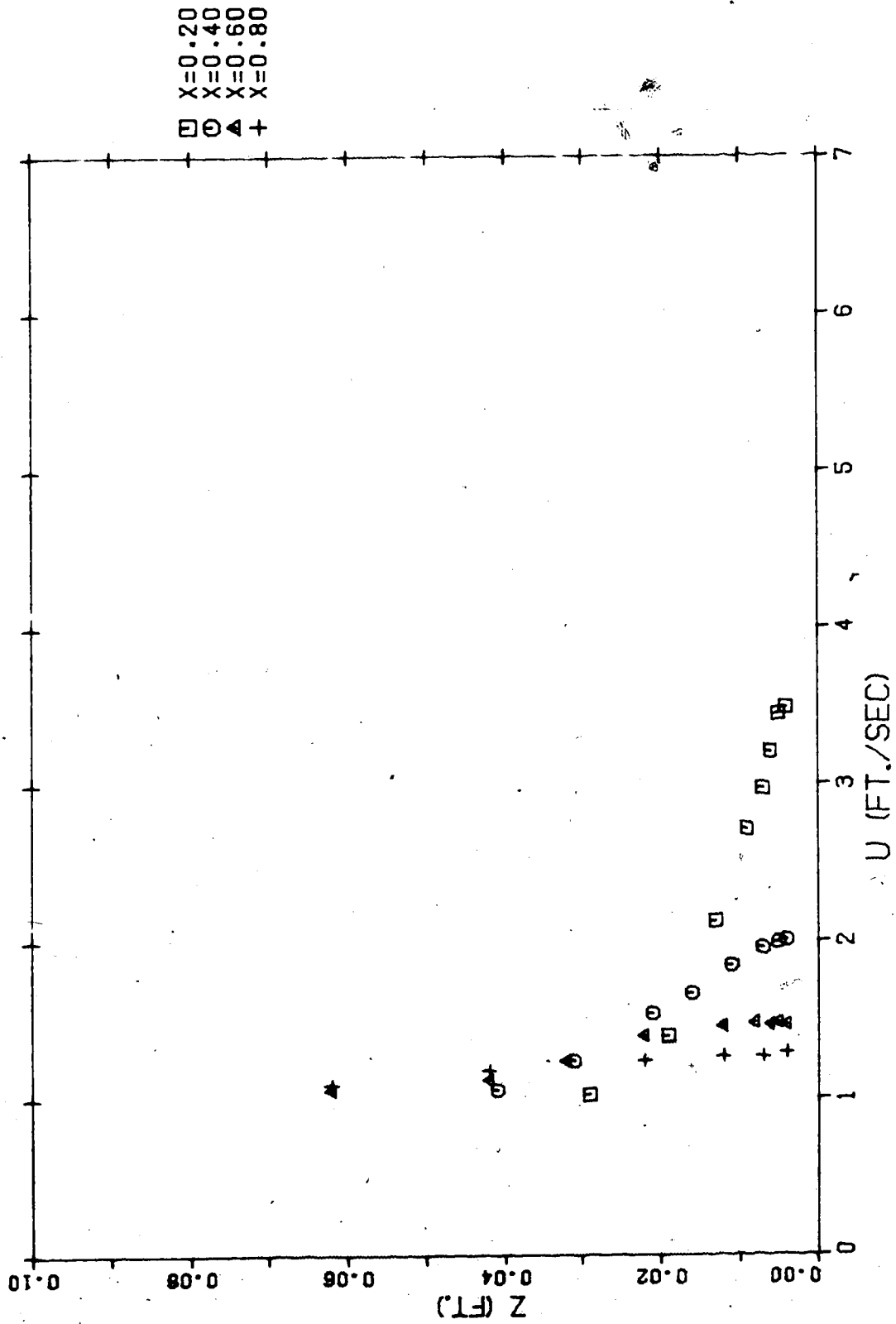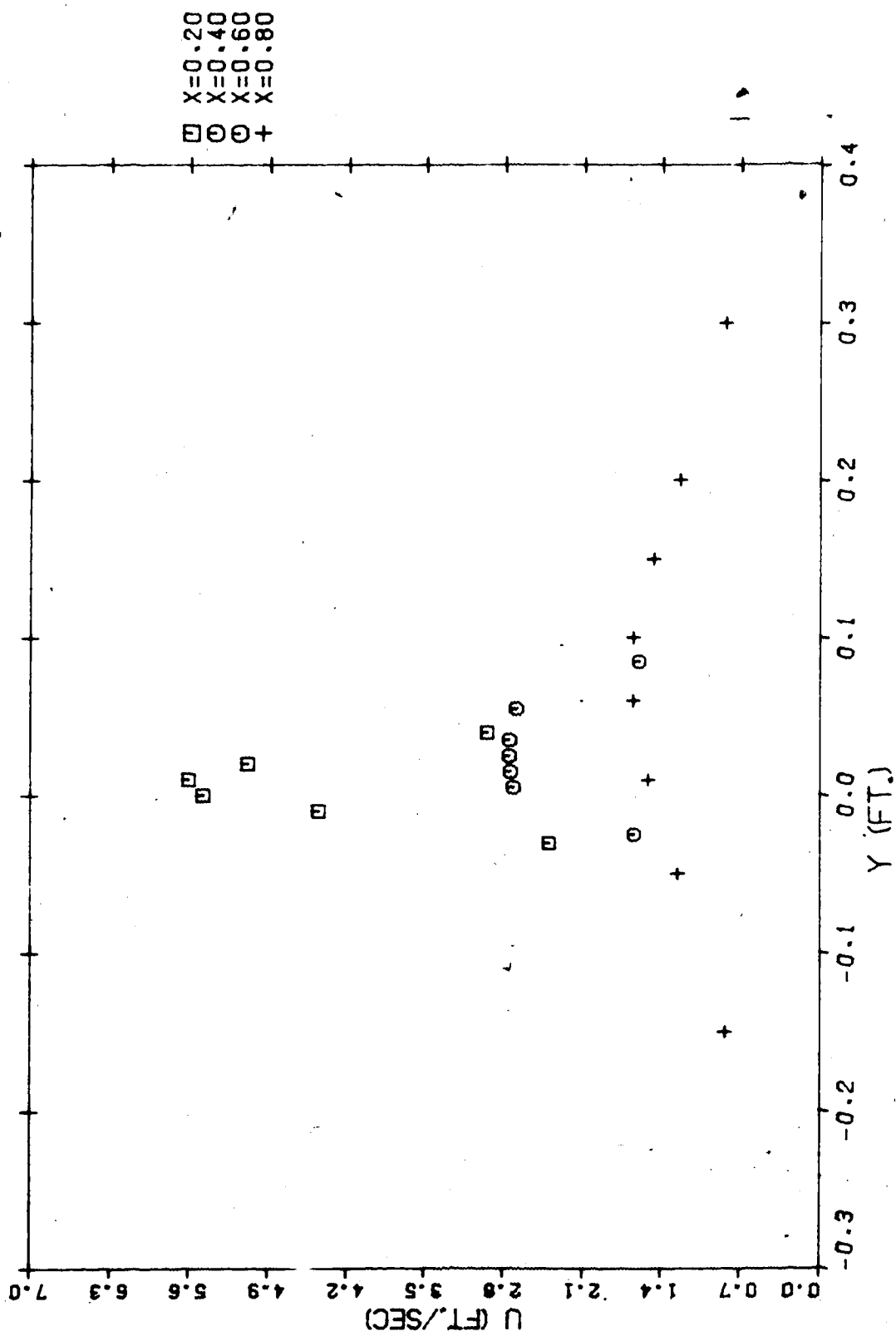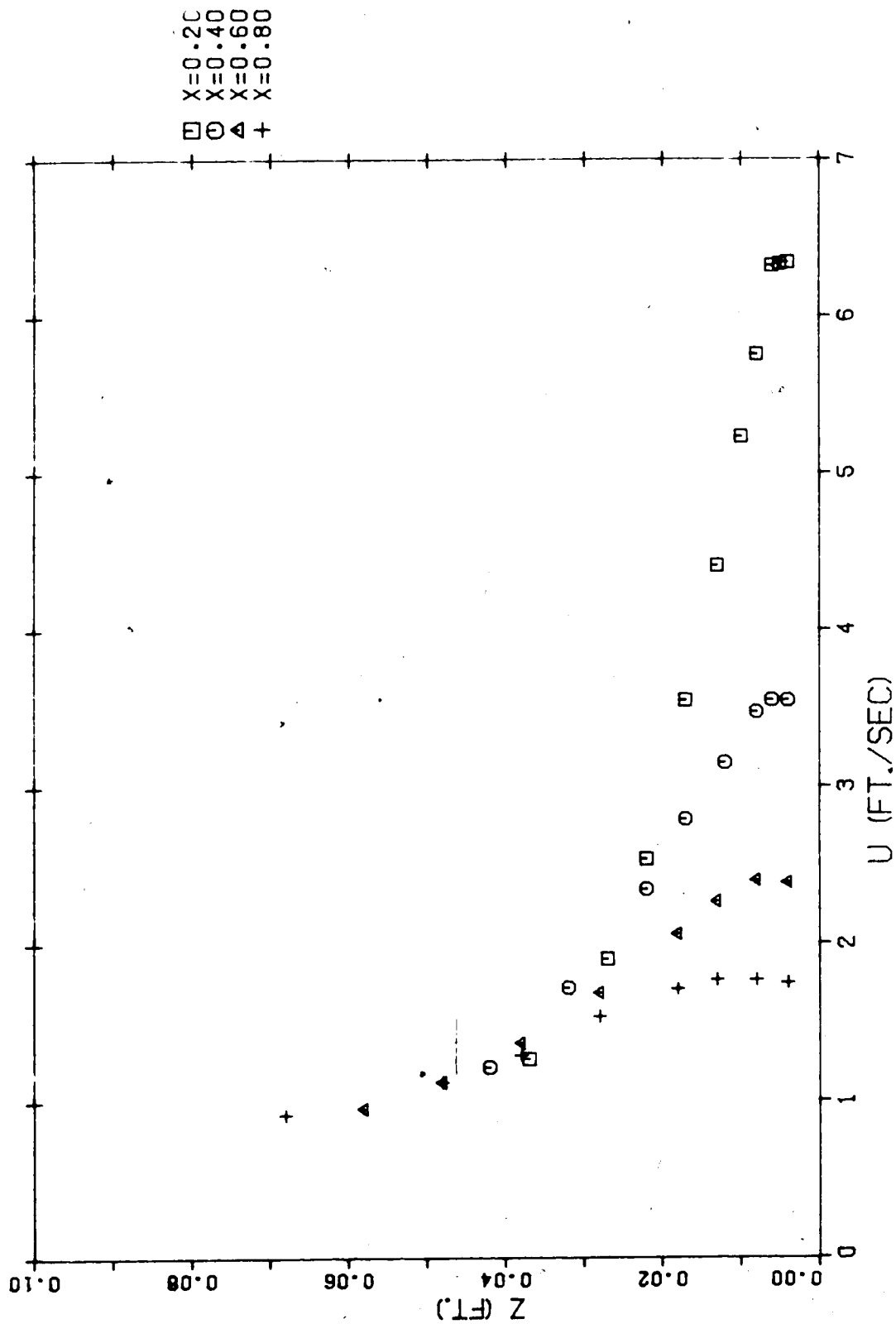
Figure 11 - Run 4 Vertical Profiles of Longitudinal Velocity
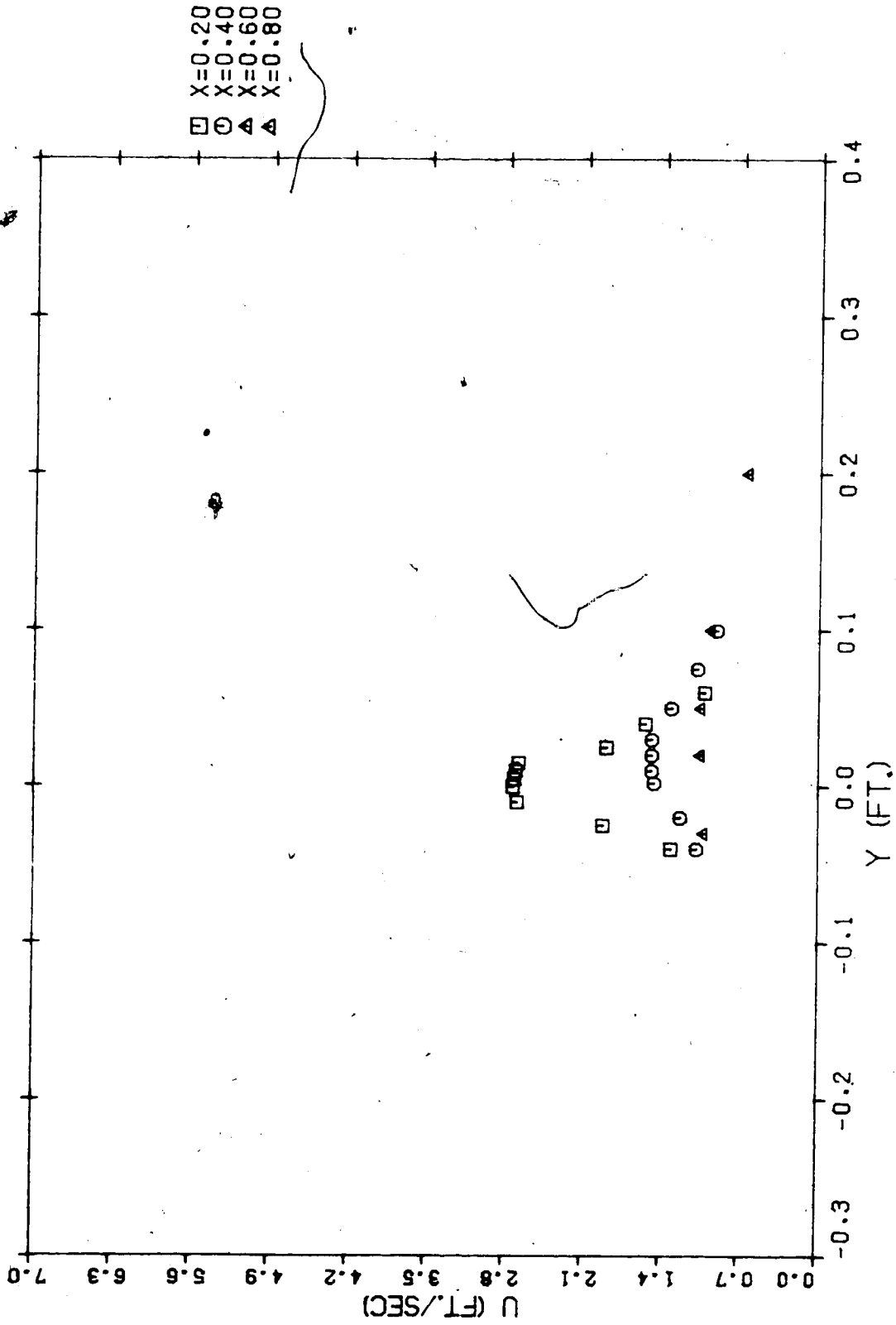
Figure 12 - Run 5 Lateral Profiles of Longitudinal Velocity
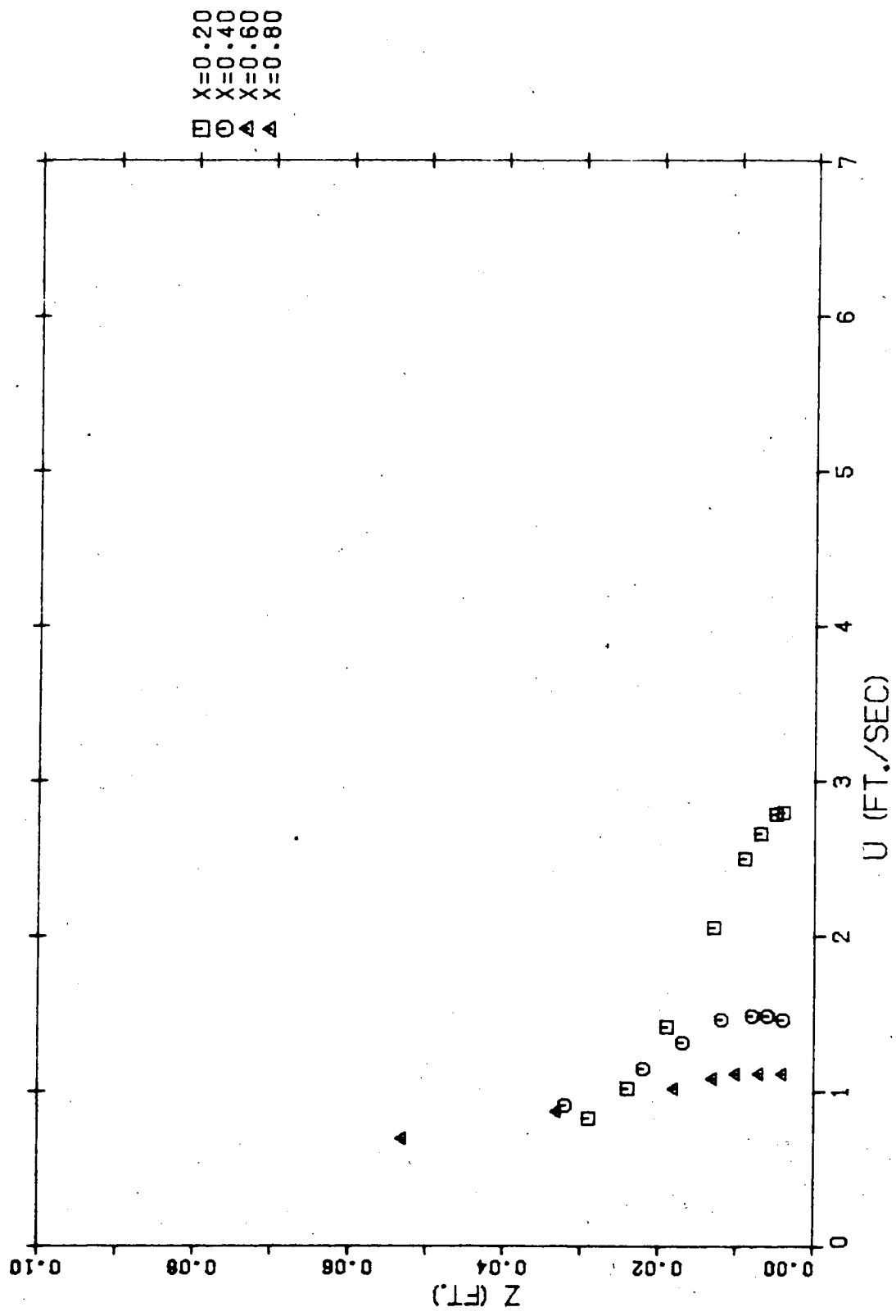
Figure 13 - Run 5 Vertical Profiles of Longitudinal Velocity
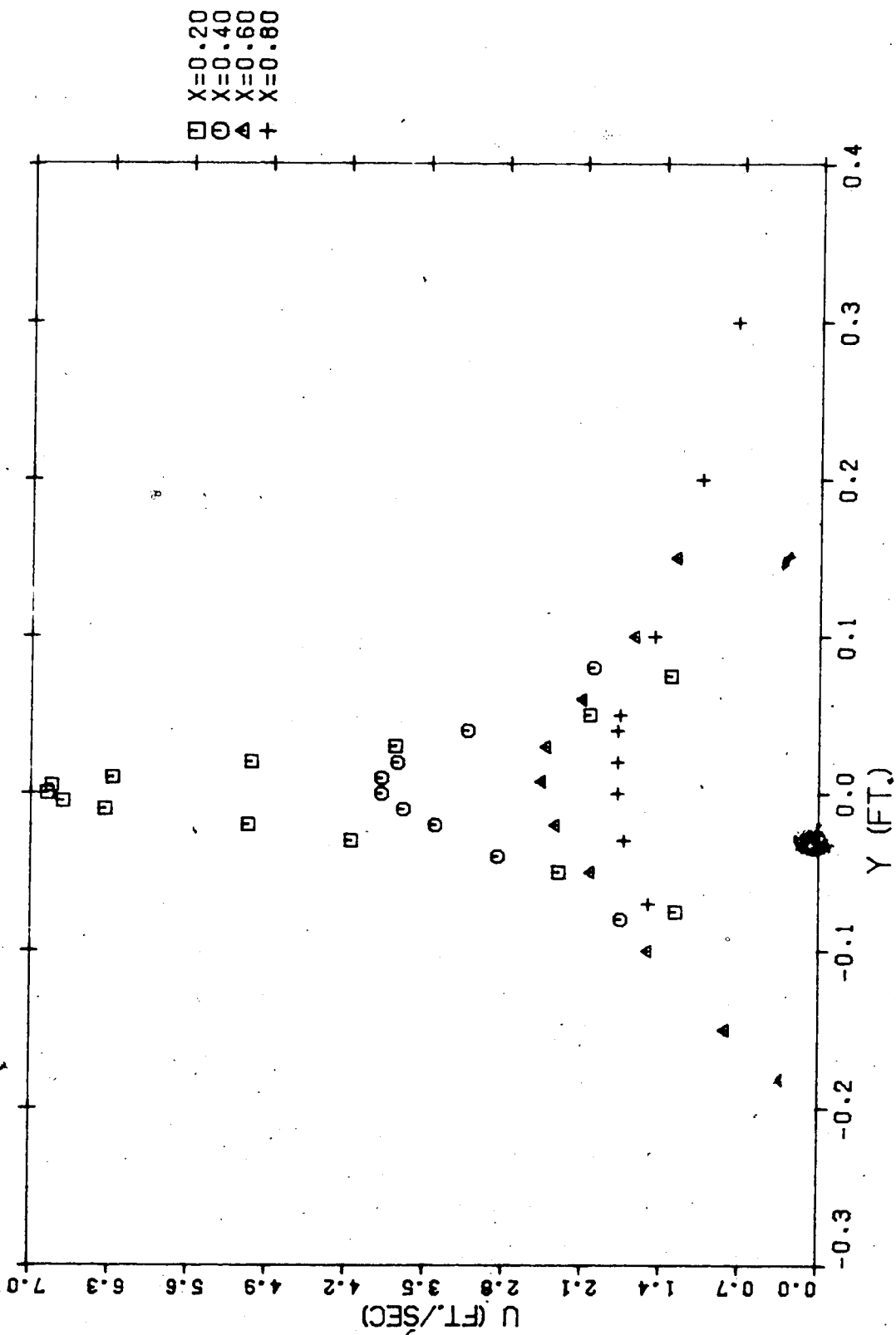
Figure 14 - Run 6 Lateral Profiles of Longitudinal Velocity
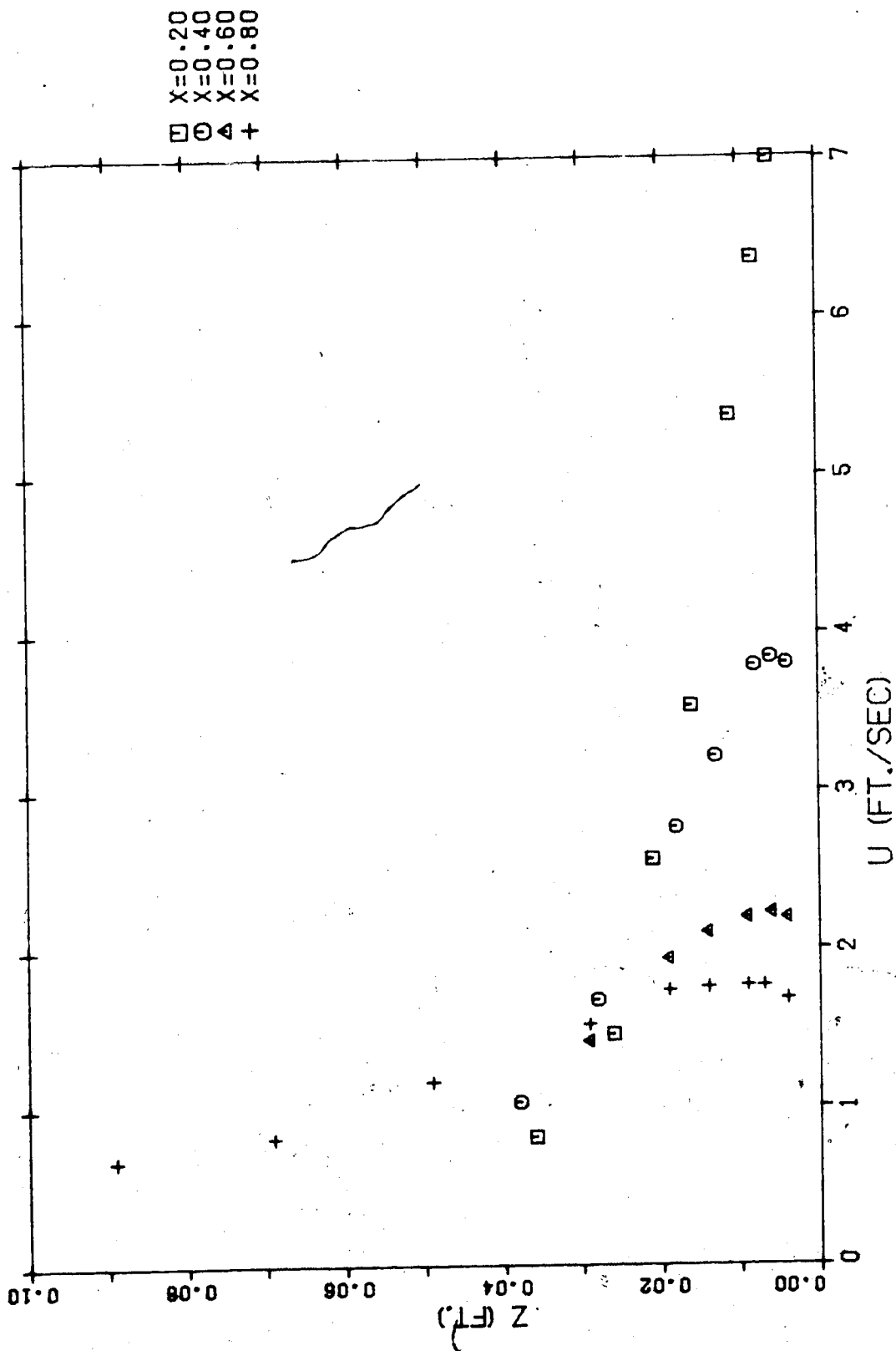
Figure 15 - Run 6 Vertical Profiles of Longitudinal Velocity

1.2 Analysis of Experiments

1.2.1 Methodology

To reduce the experimental data to a managable and useful form, similarity analysis was applied. Practicaly, this involved plotting each profile, fitting a smooth curve through the data points and then extracting the pertinent scales. The scales needed were maximum velocity, distance of maximum velocity from origin, and distance from point of maximimum velocity to the point where the velocity was one half maximum. In the case of lateral profiles the latter scale was measured in both directions and an average taken.

Using these scales, which were unique to any one profile, the similarity profiles of each run were plotted together and were indeed found to be similar. Figures (16) - (27) show these similarity plots for all the runs. The solid line is the often used exponential curve:

$$\frac{u}{u_m} = e^{-.693\eta^2} \tag{4}$$
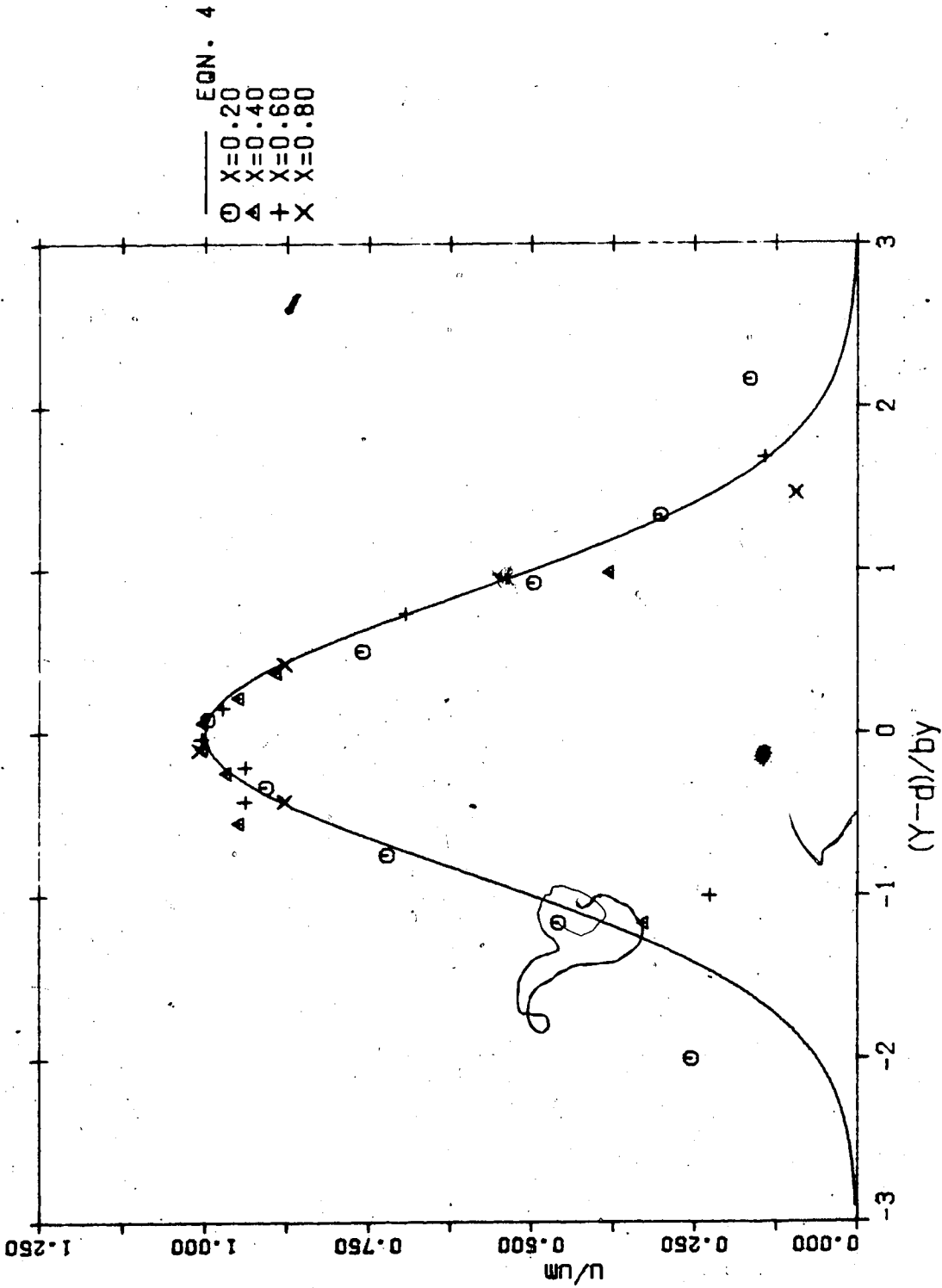
Figure 16 - Lateral Similarity Profile of Longitudinal
Velocity Run 1
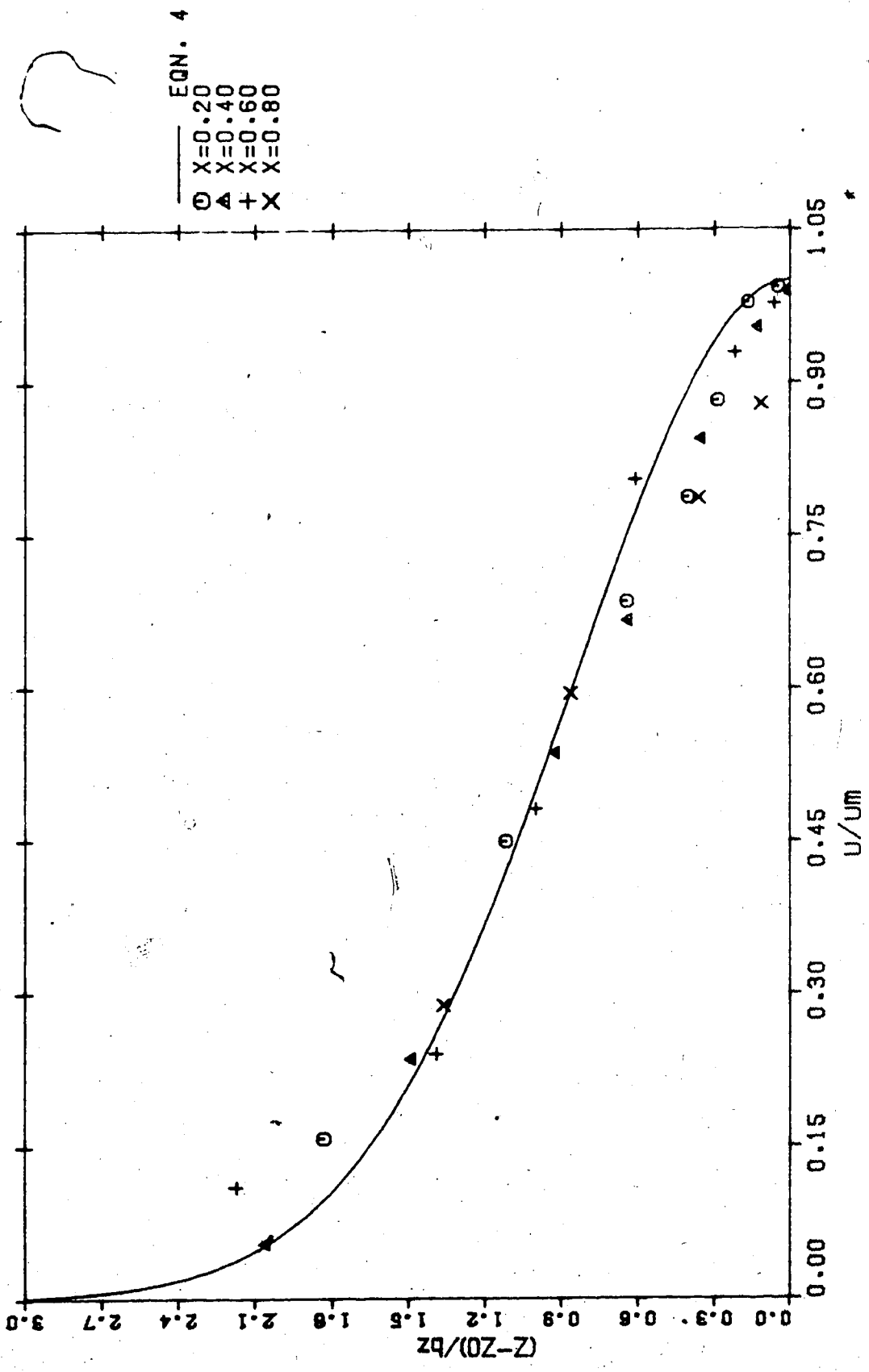
Figure 17 - Vertical Similarity Profile of Longitudinal
Velocity Run 1
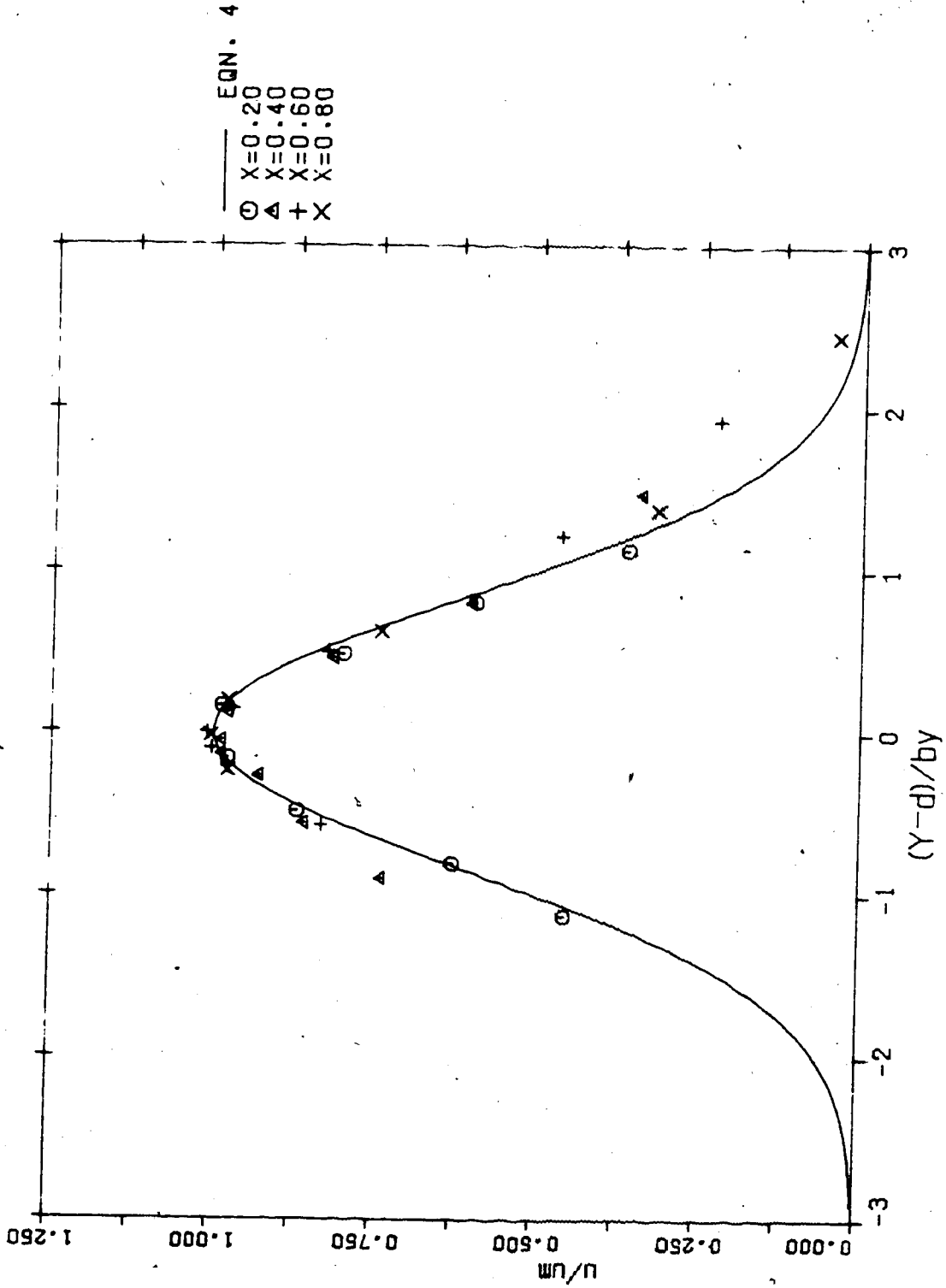
Figure 20 - Lateral Similarity Profile of Longitudinal
Velocity Run 3
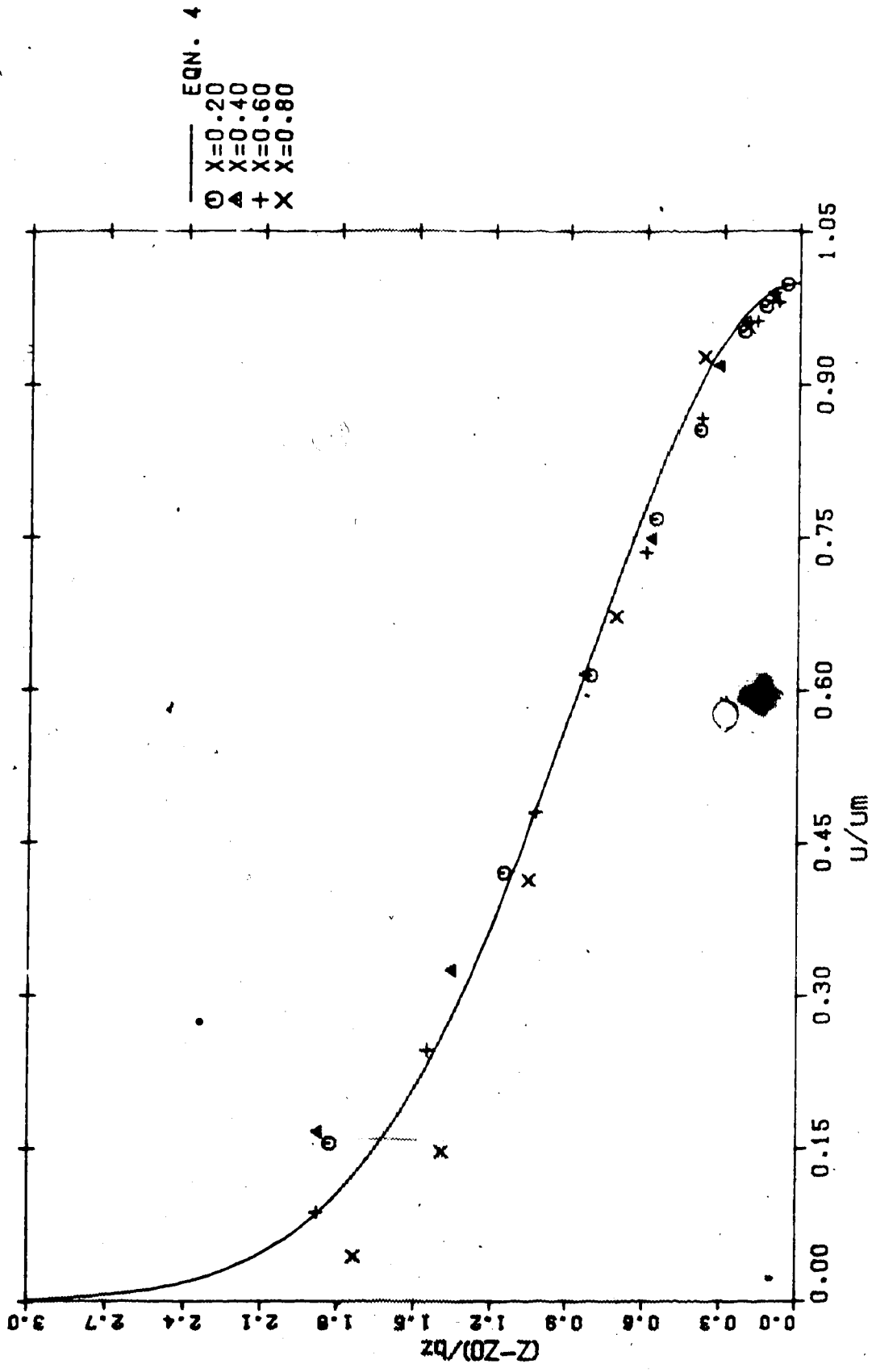
Figure 21 - Vertical Similarity Profile of Longitudinal
Velocity Run 3
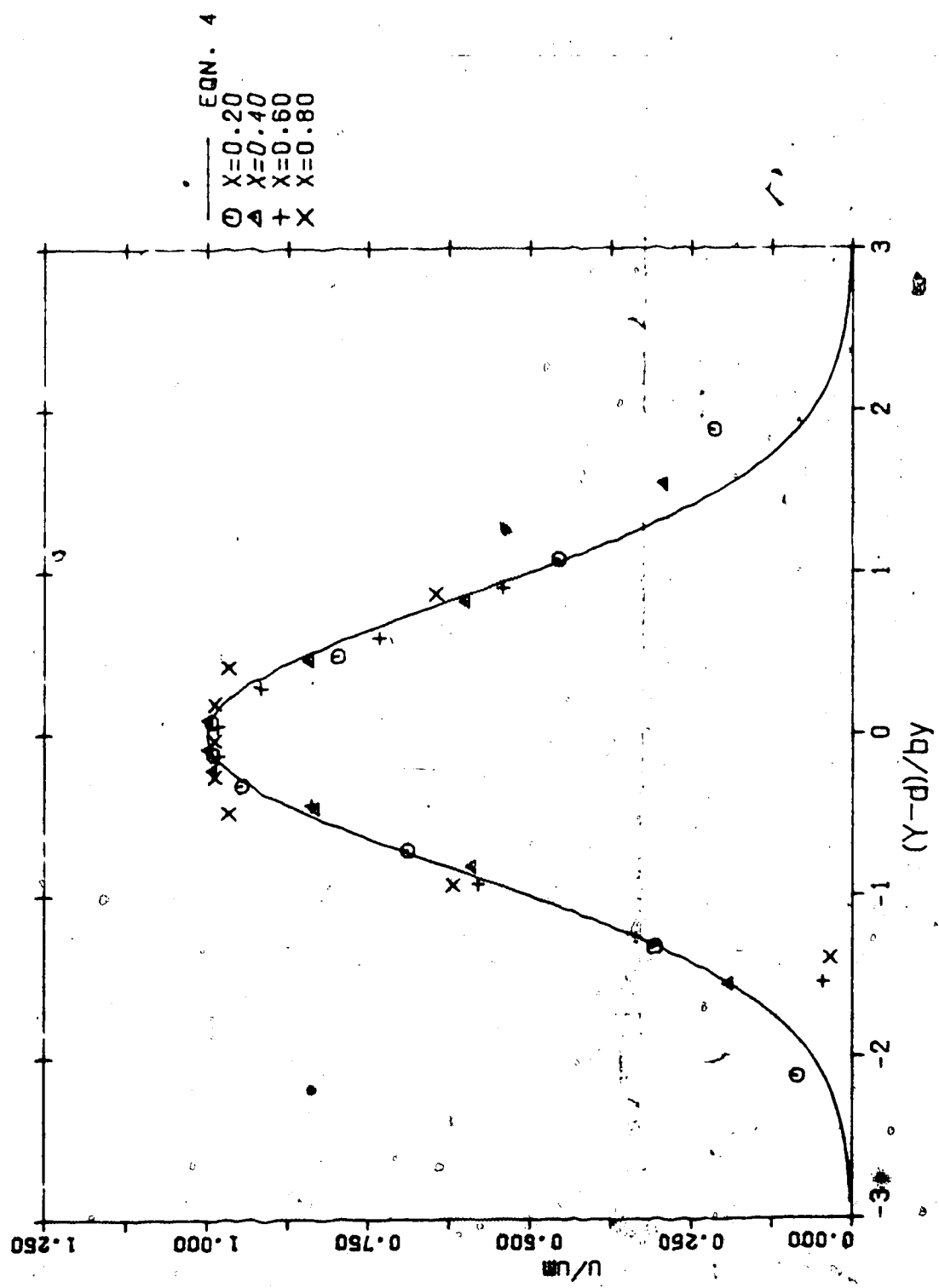
Figure 22 - Lateral Similarity Profile of Longitudinal
Velocity Run 4

41
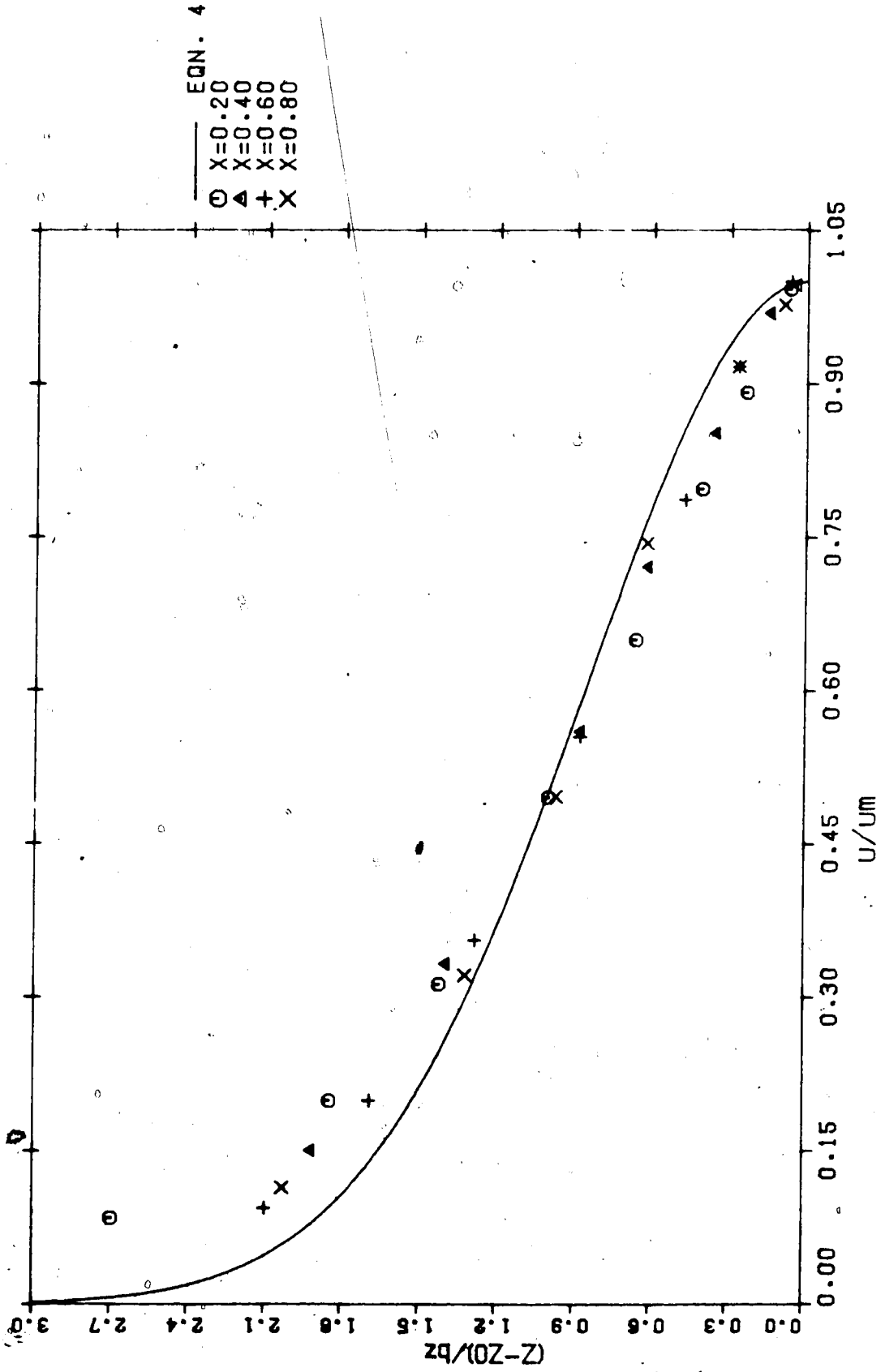
Figure 23 - Vertical Similarity Profile of Longitudinal
Velocity Run 4
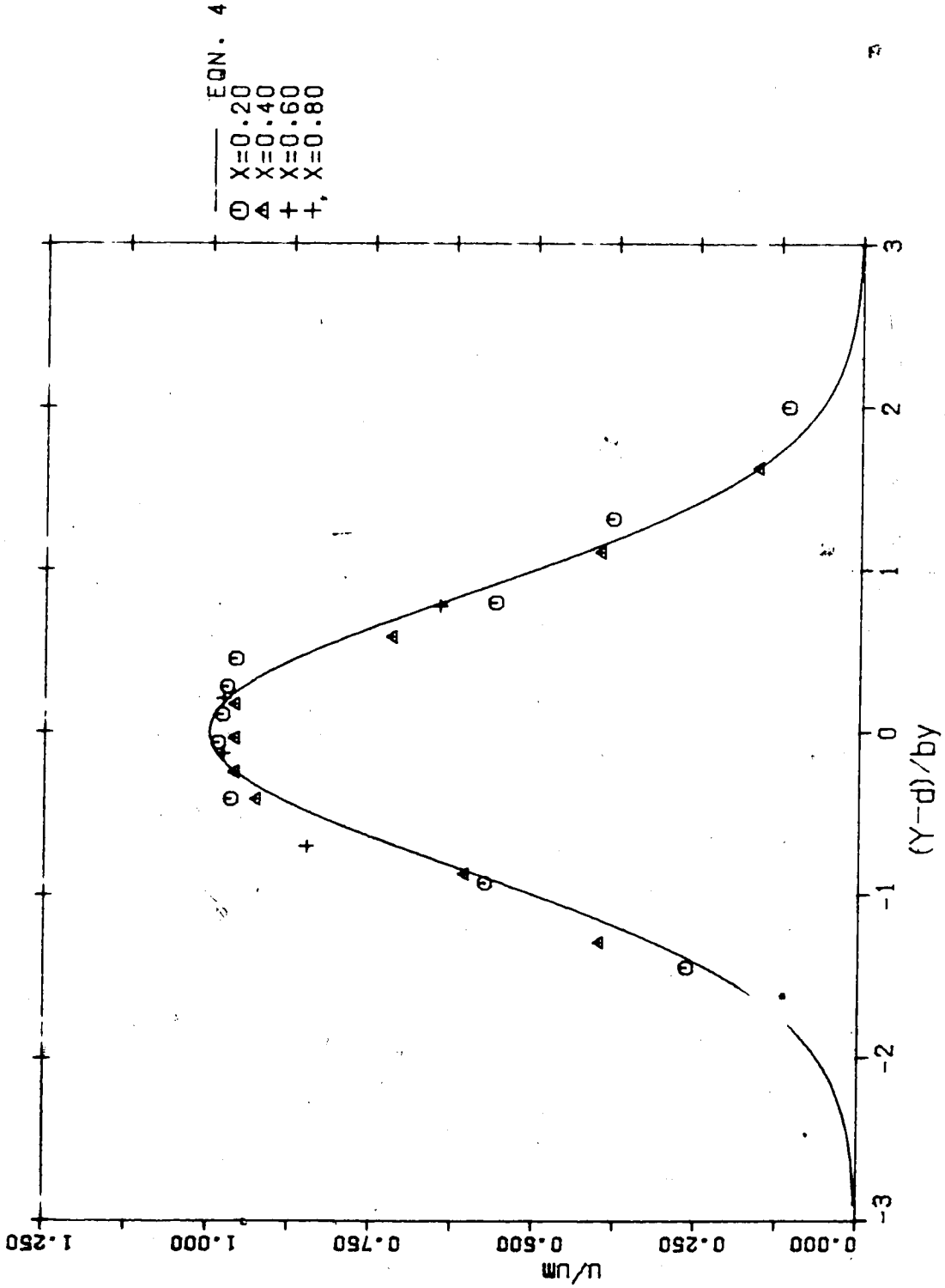
Figure 24 - Lateral Similarity Profile of Longitudinal
Velocity Run 5
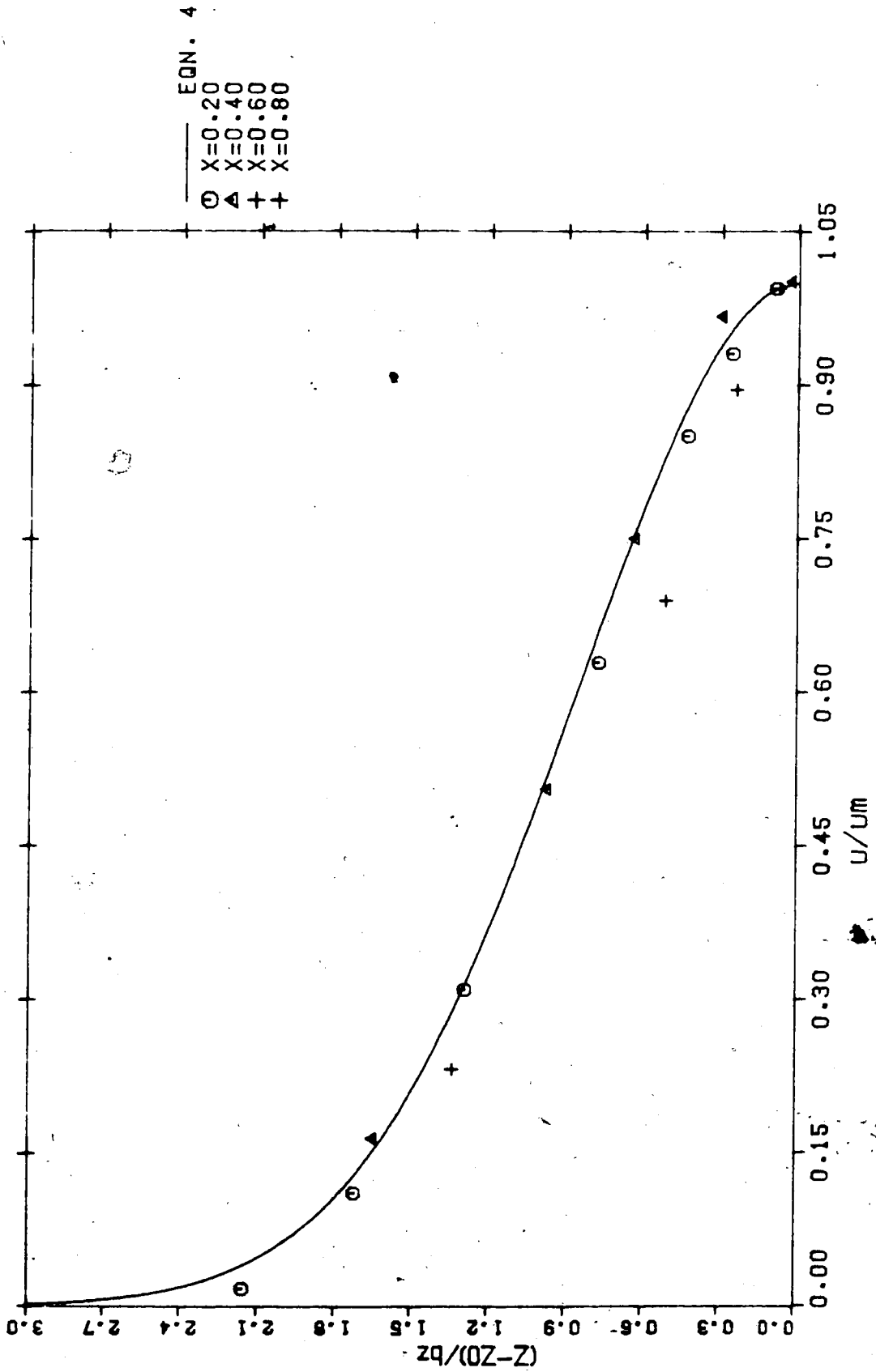
Figure 25 - Vertical Similarity Profile of Longitudinal
Velocity Run 5
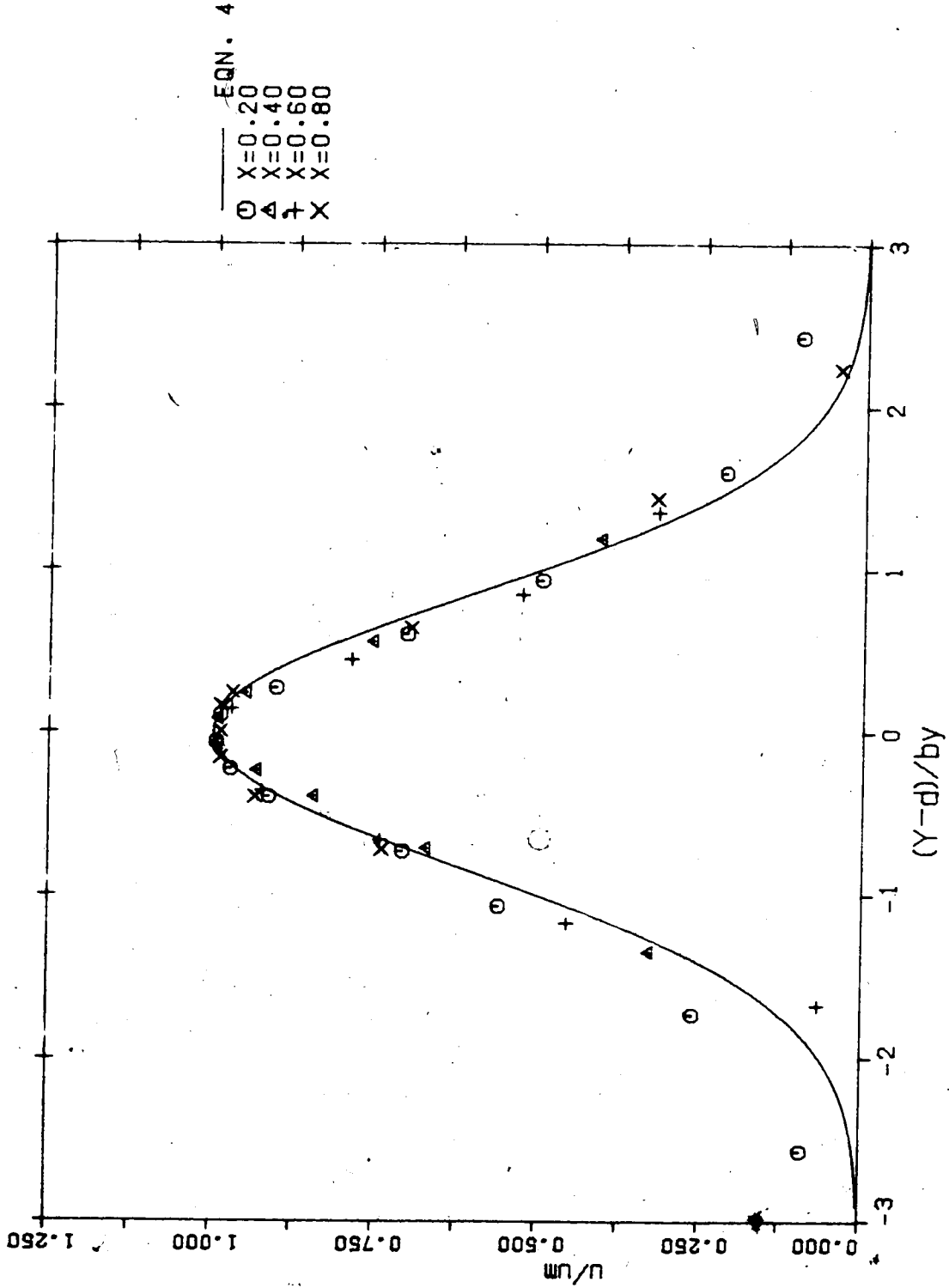
Figure 26 - Lateral Similarity Profile of Longitudinal Velocity Run 6
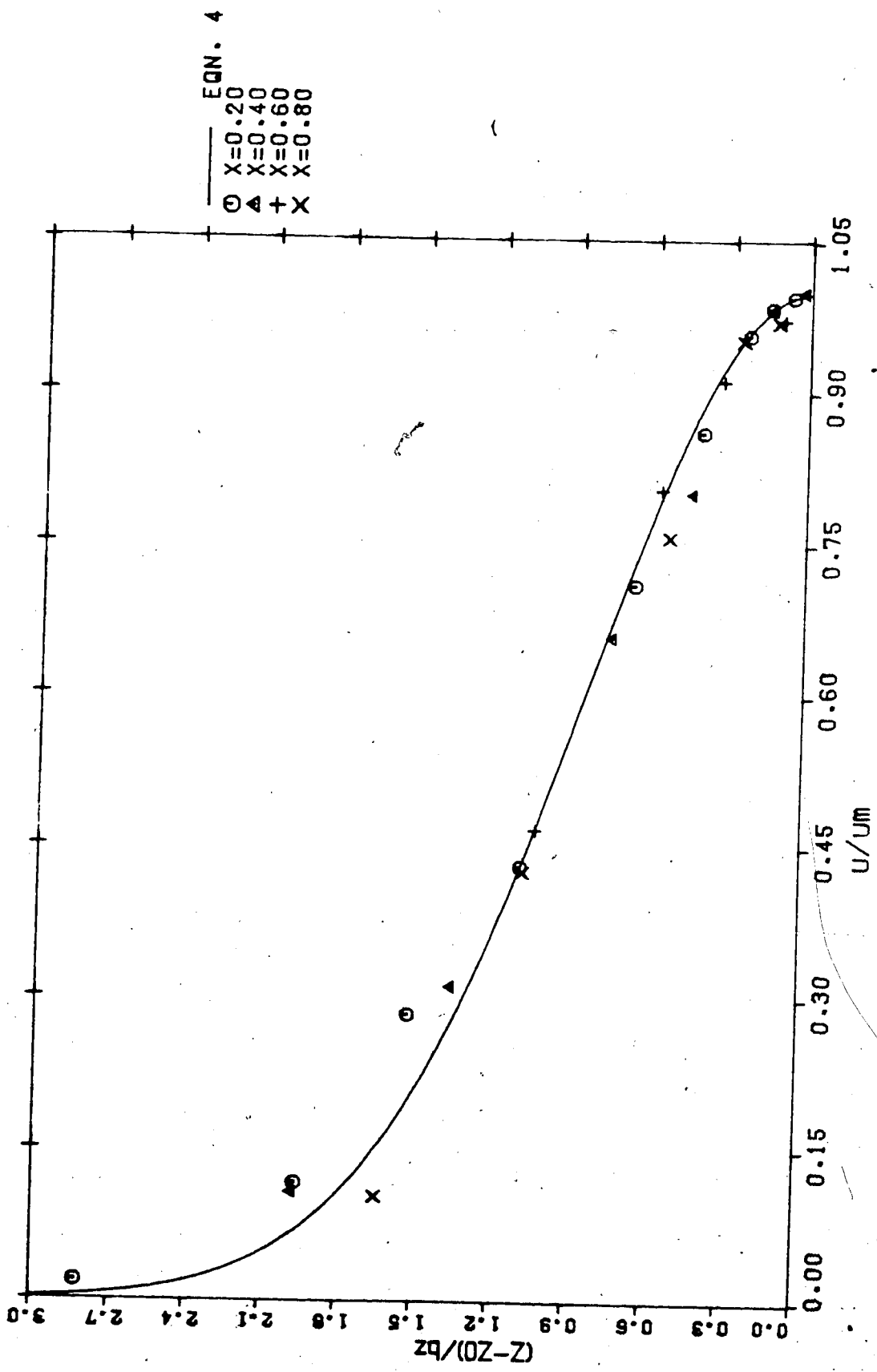
Figure 27 - Vertical Similarity Profile of Longitudinal
Velocity Run 6

1.2.2 Scale Analysis

The velocity data, having been shown to have similar profiles, were next analysed with respect to the variation of their scales. Figures (28) - (32) show graphically the downstream variation of each of the scales for all of the runs. In order to correlate these scale variations reference was made to the compound jet theory briefly discussed above. Using U as a velocity scale and the momentum thickness - to nondimensionalise the profile scales, figures (33) - (37) were plotted and show reasonably good corelation. The results of Stalker(1979) are shown for comparison. The velocity correlation agrees very well while the length scale predictions do not. This is believed to have been caused by the small density difference between the jet and ambient flow which resulted in a flatter, wider jet profile in the present study.
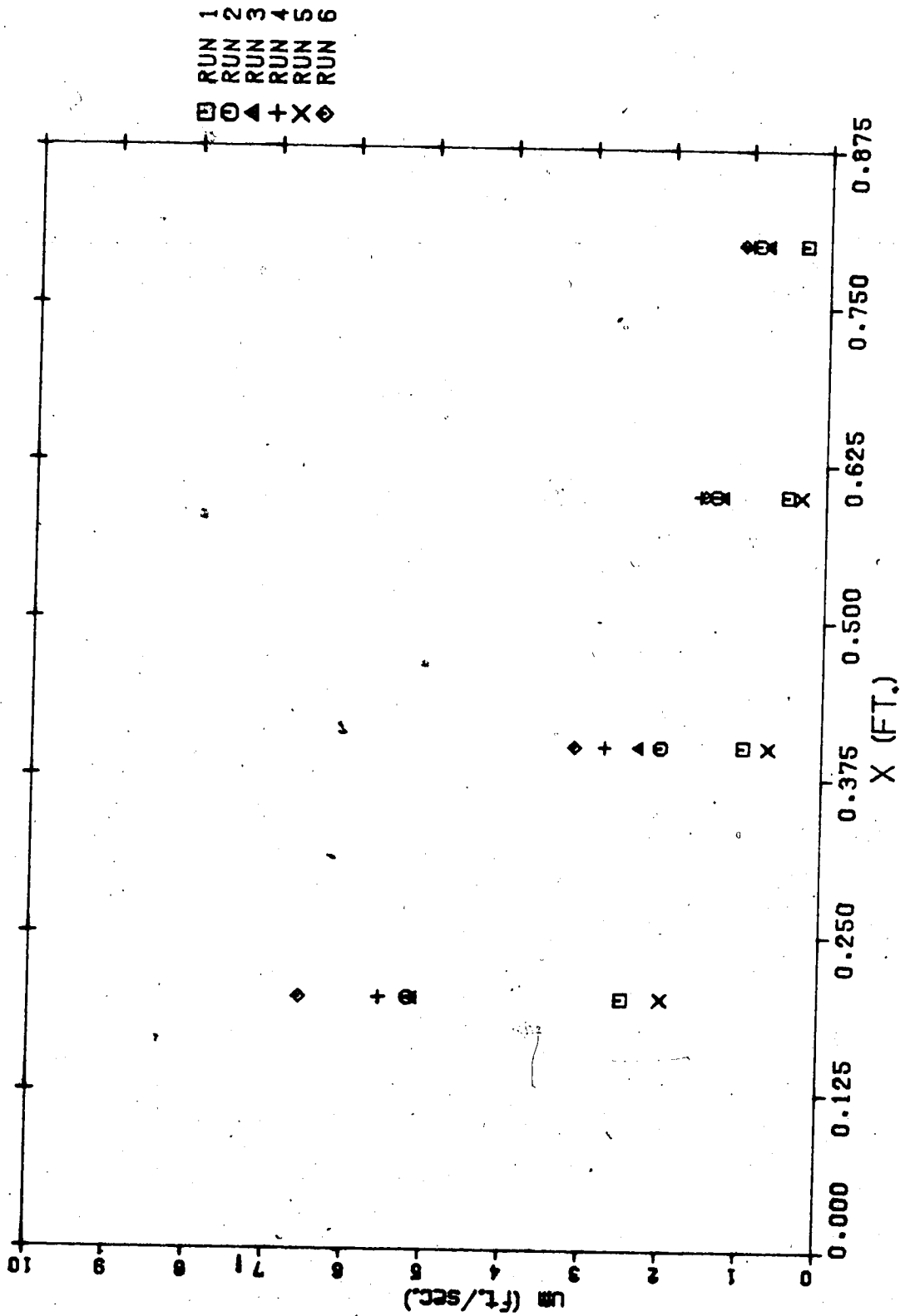
Figure 28 - Variation of Maximum Velocity - Circular Wall Jets in Curved Channel Flow
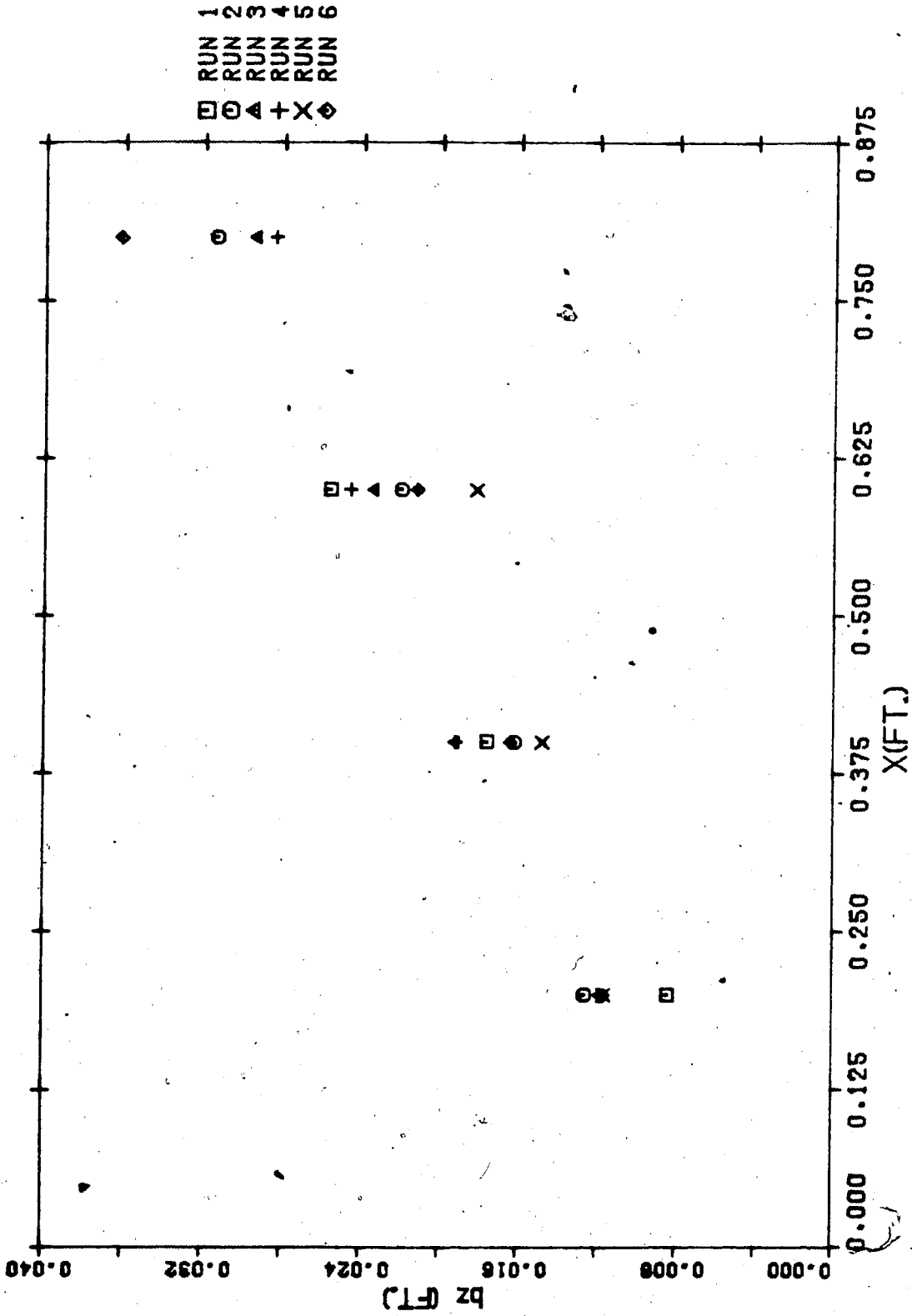
Figure 29 - Variation of Vertical Length Scale - Circular
Wall Jets in Curved Channel Flow
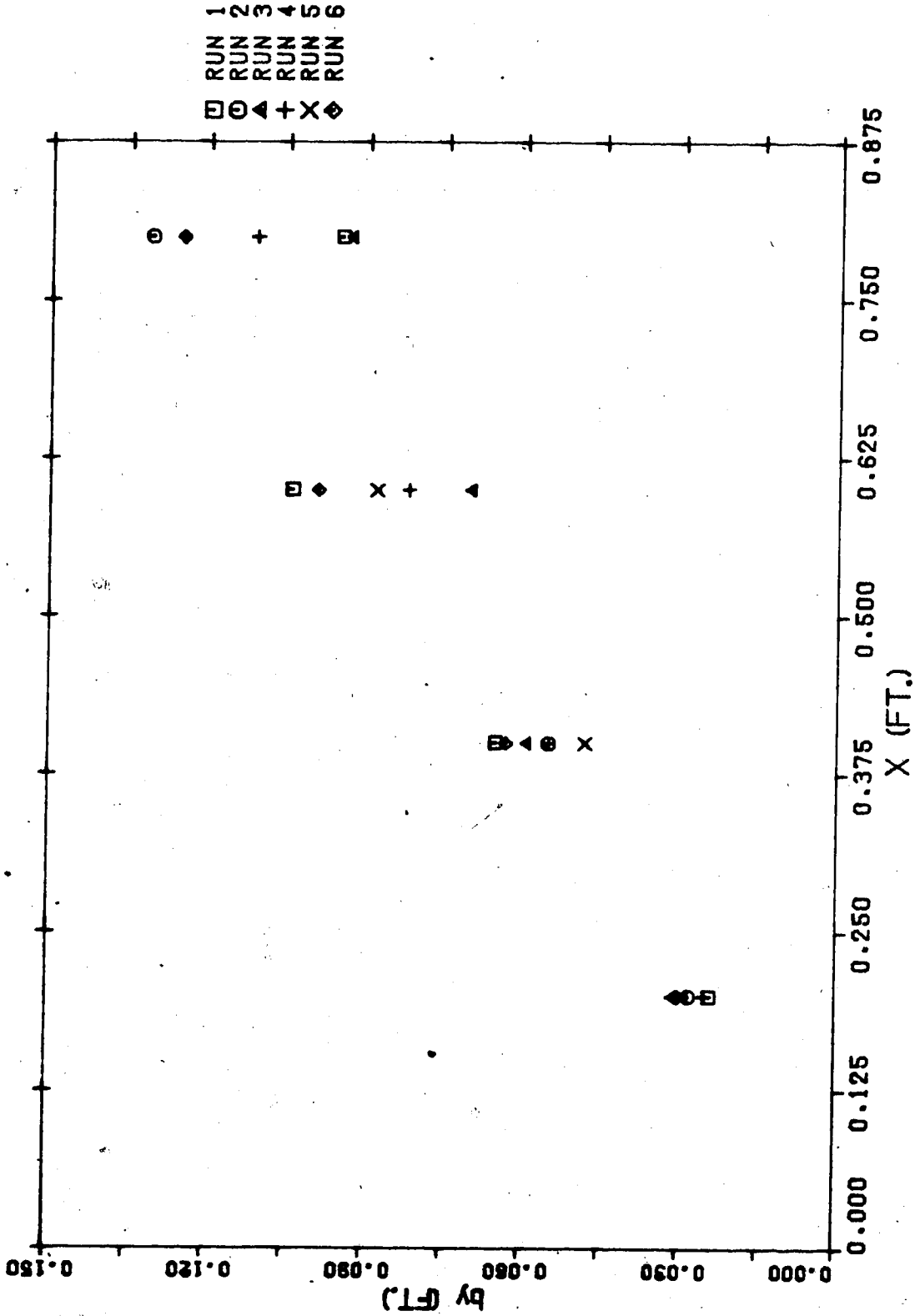
Figure 30 - Variation of Lateral Length Scale - Circular
Wall Jets in Curved Channel Flow
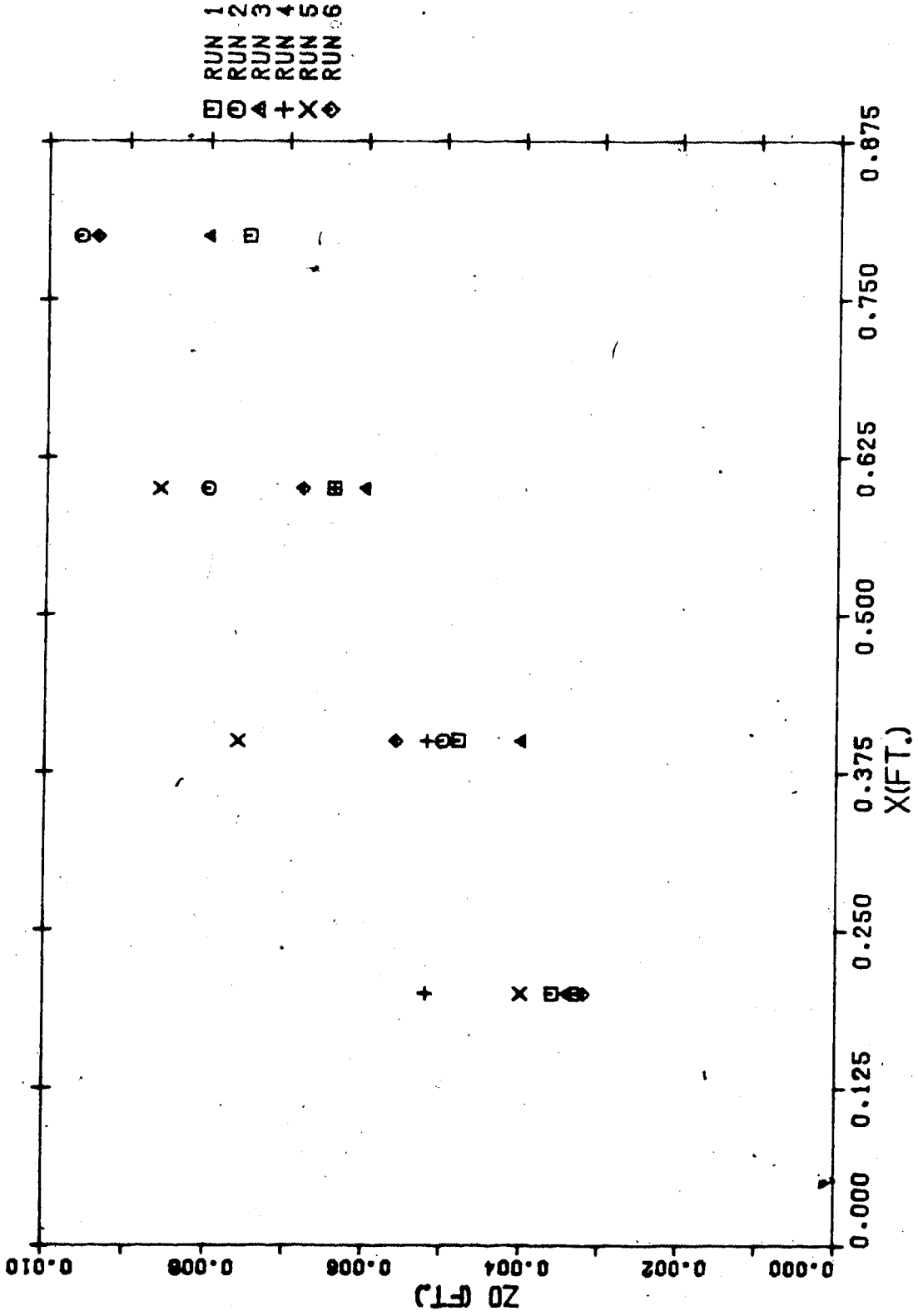
Figure 31 - Variation of Boundary Layer Thickness - Circular
Wall Jets in Curved Channel Flow
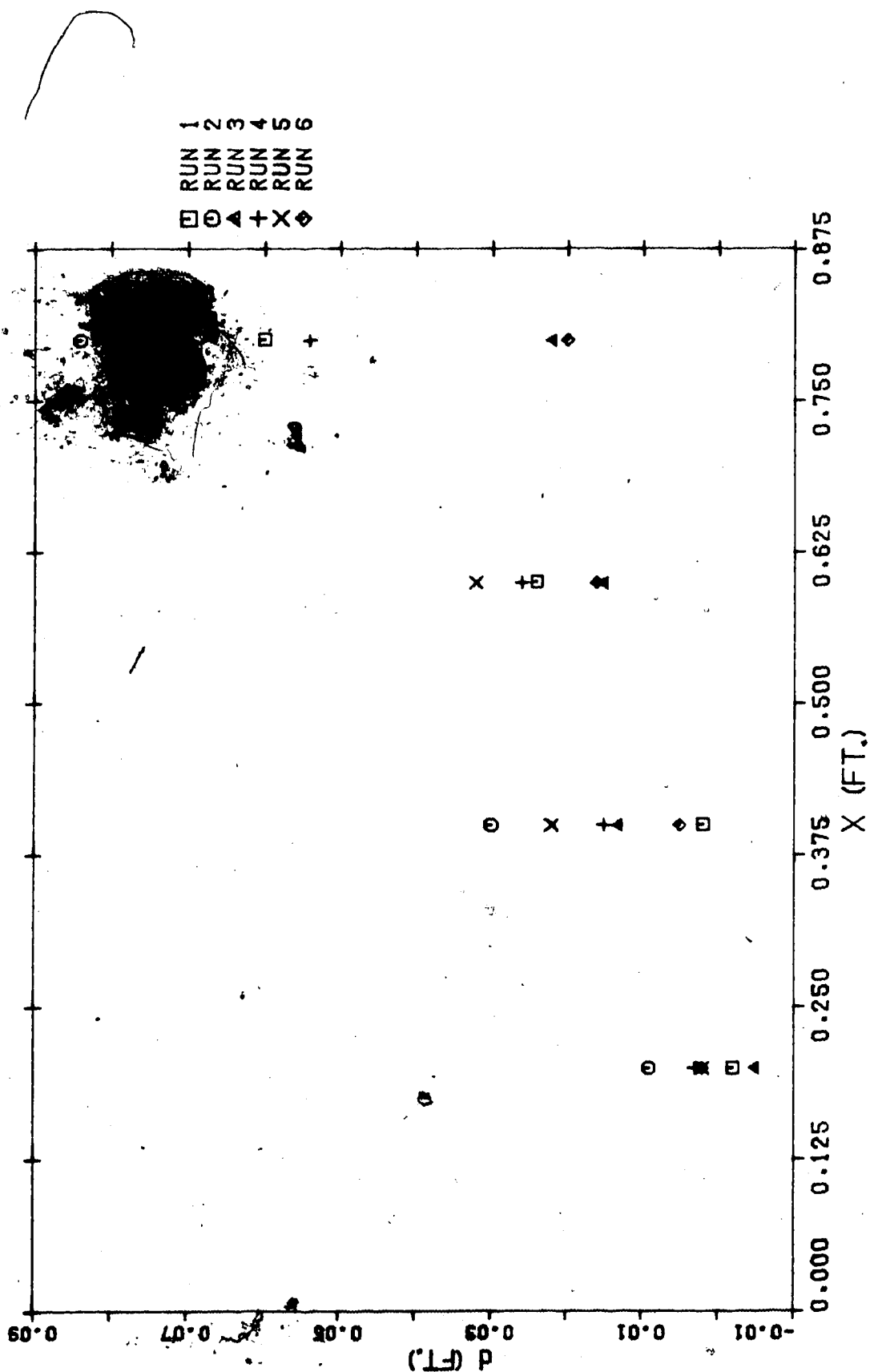
Figure 32 - Jet Deflection - Circular Wall Jets in Curved Channel Flow
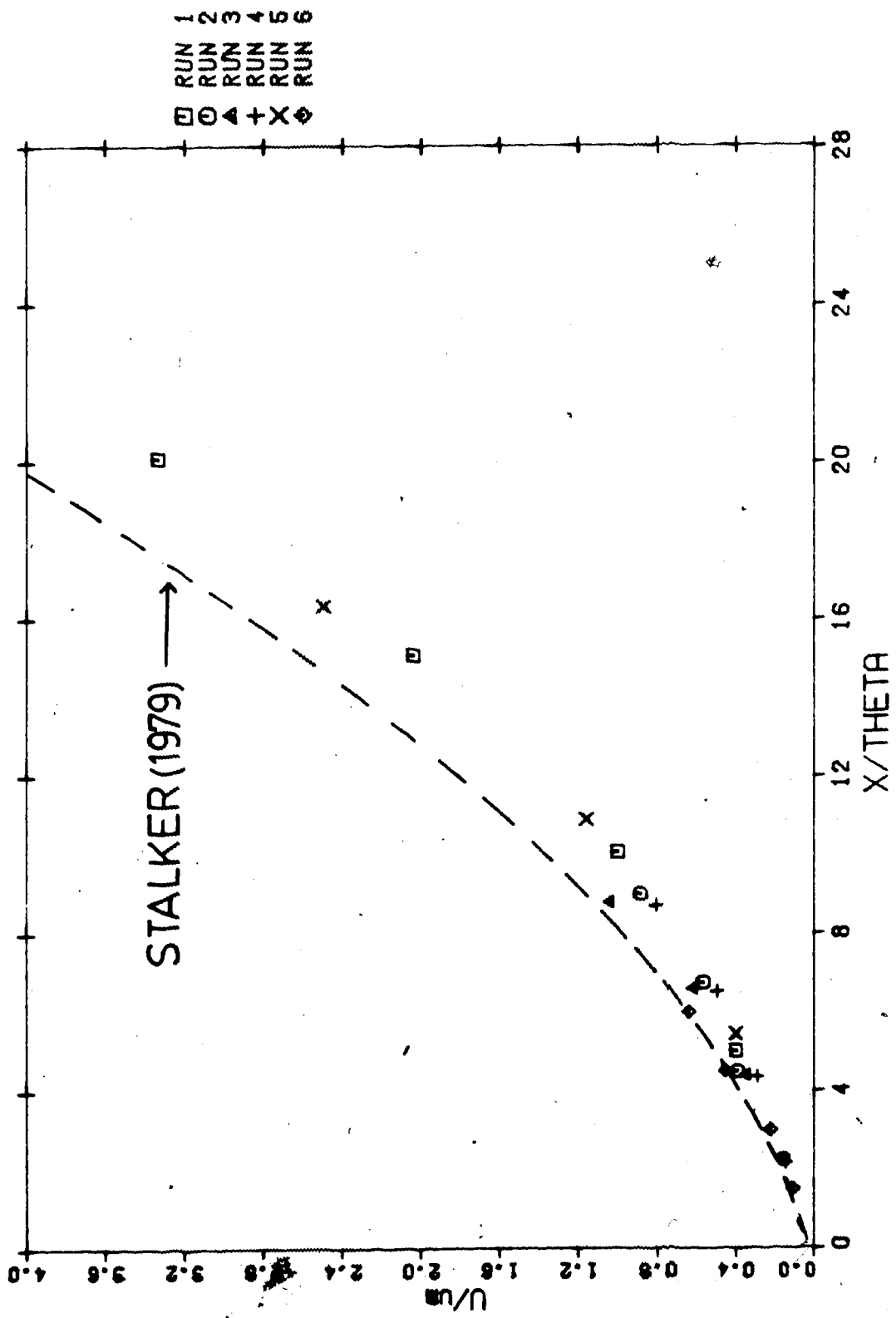
Figure 33 - Prediction of Maximum Velocity - Circular Wall
Jets in Curved Channel Flow
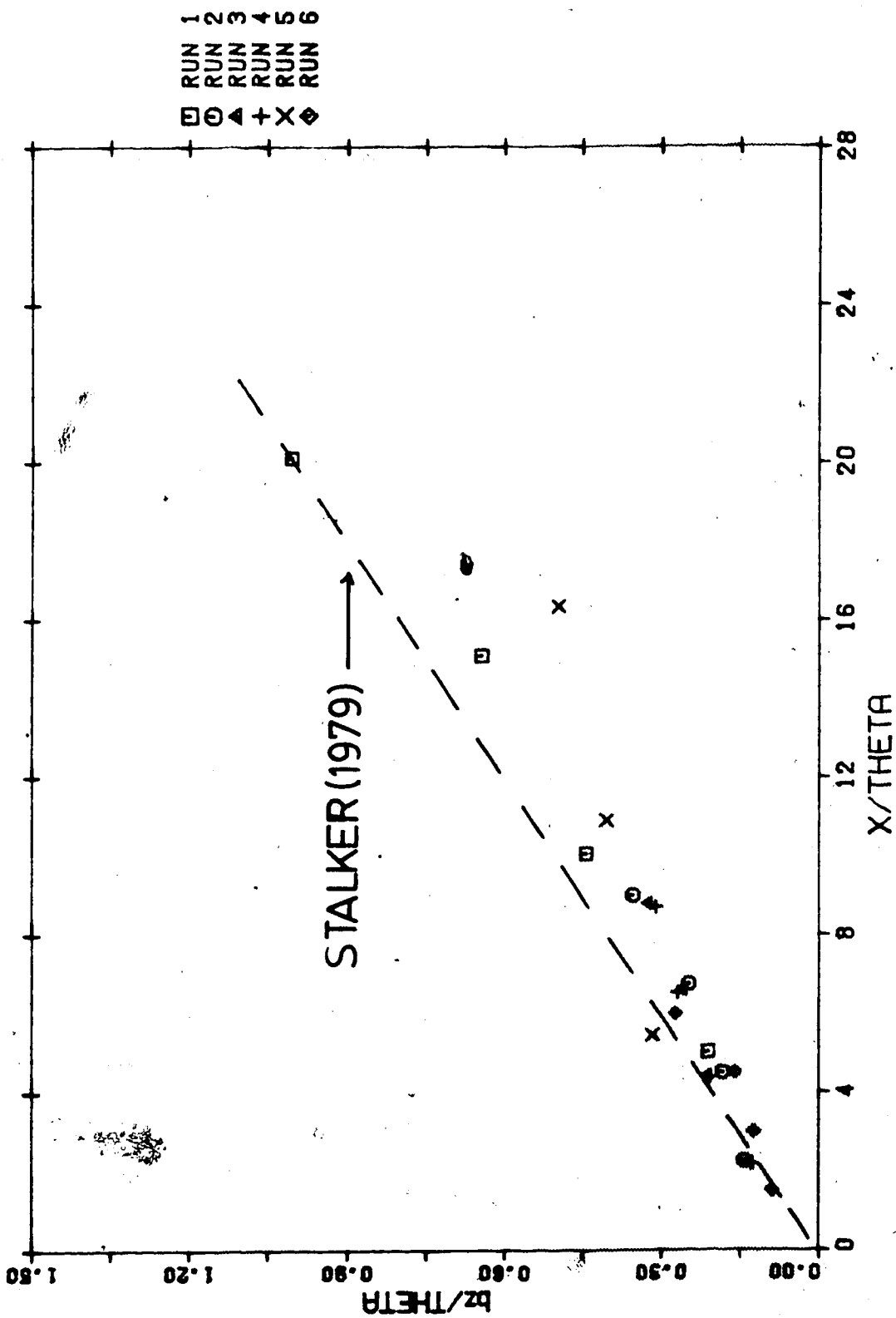
Figure 34 - Prediction of Vertical Length Scale - Circular
Wall Jets in Curved Channel Flow
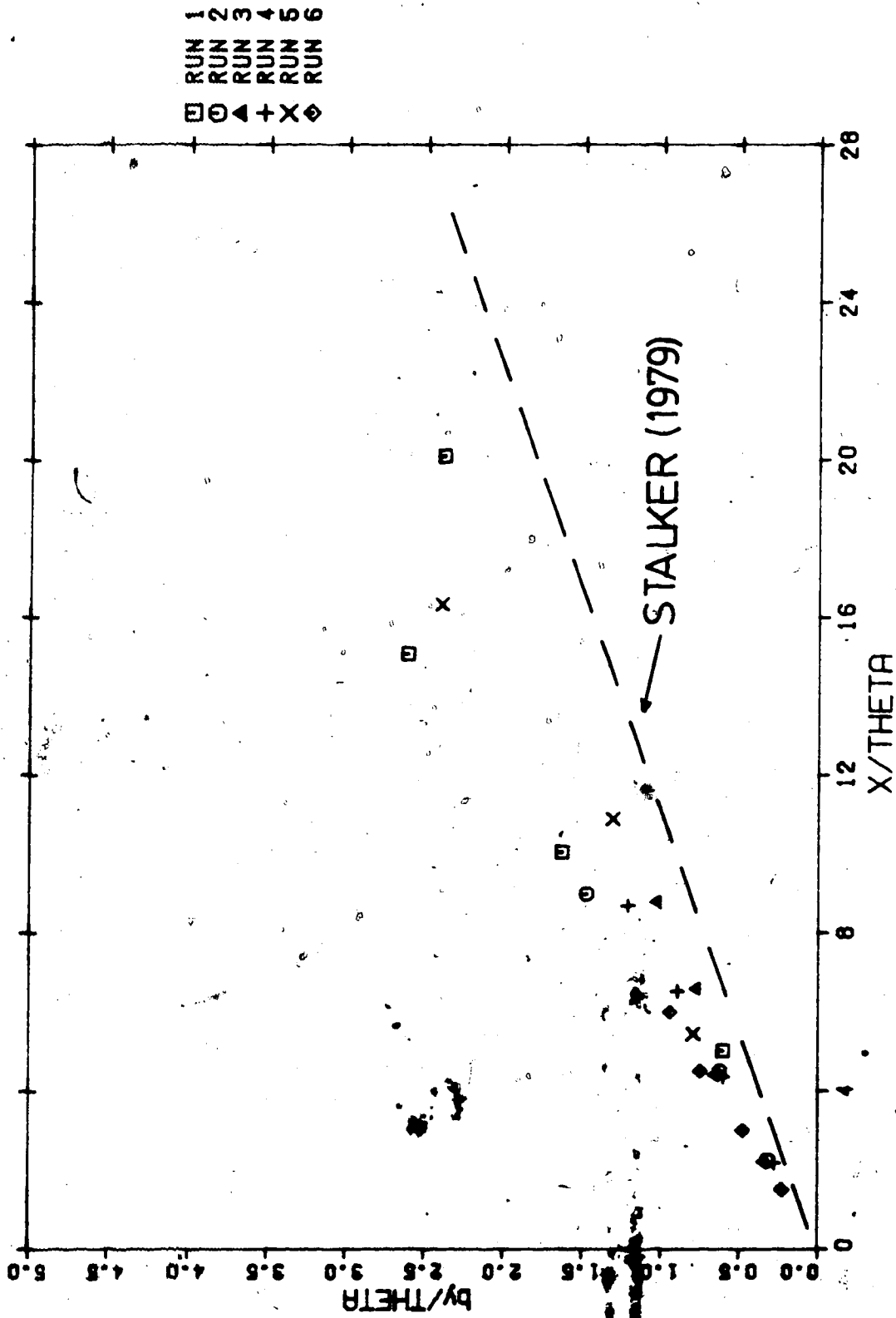
Figure 35 - Prediction of Lateral Length Scale - Circular Wall Jets in Curved Channel Flow
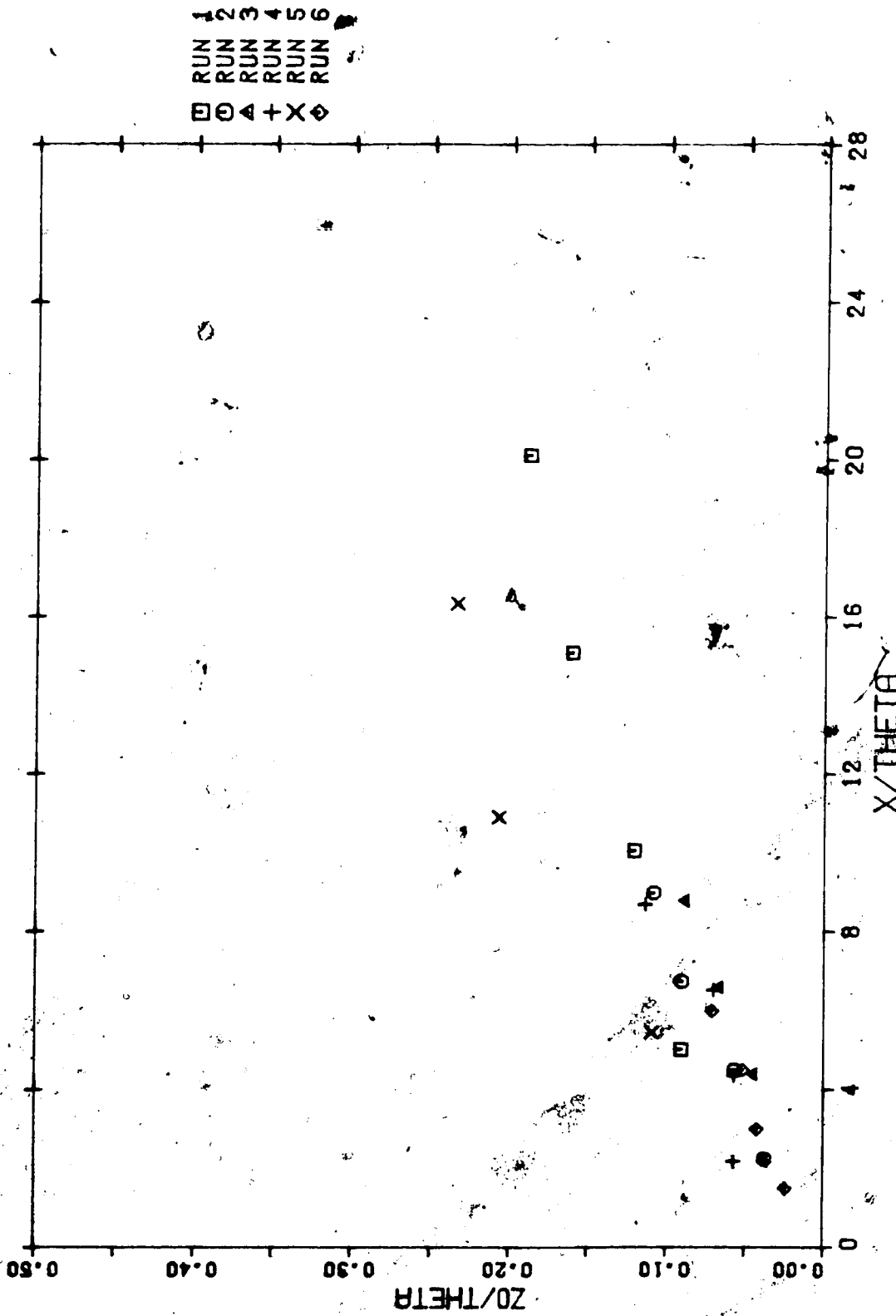
Figure 36 - Prediction of Boundary Layer Thickness - Circular Wall Jets in Curved Channel Flow
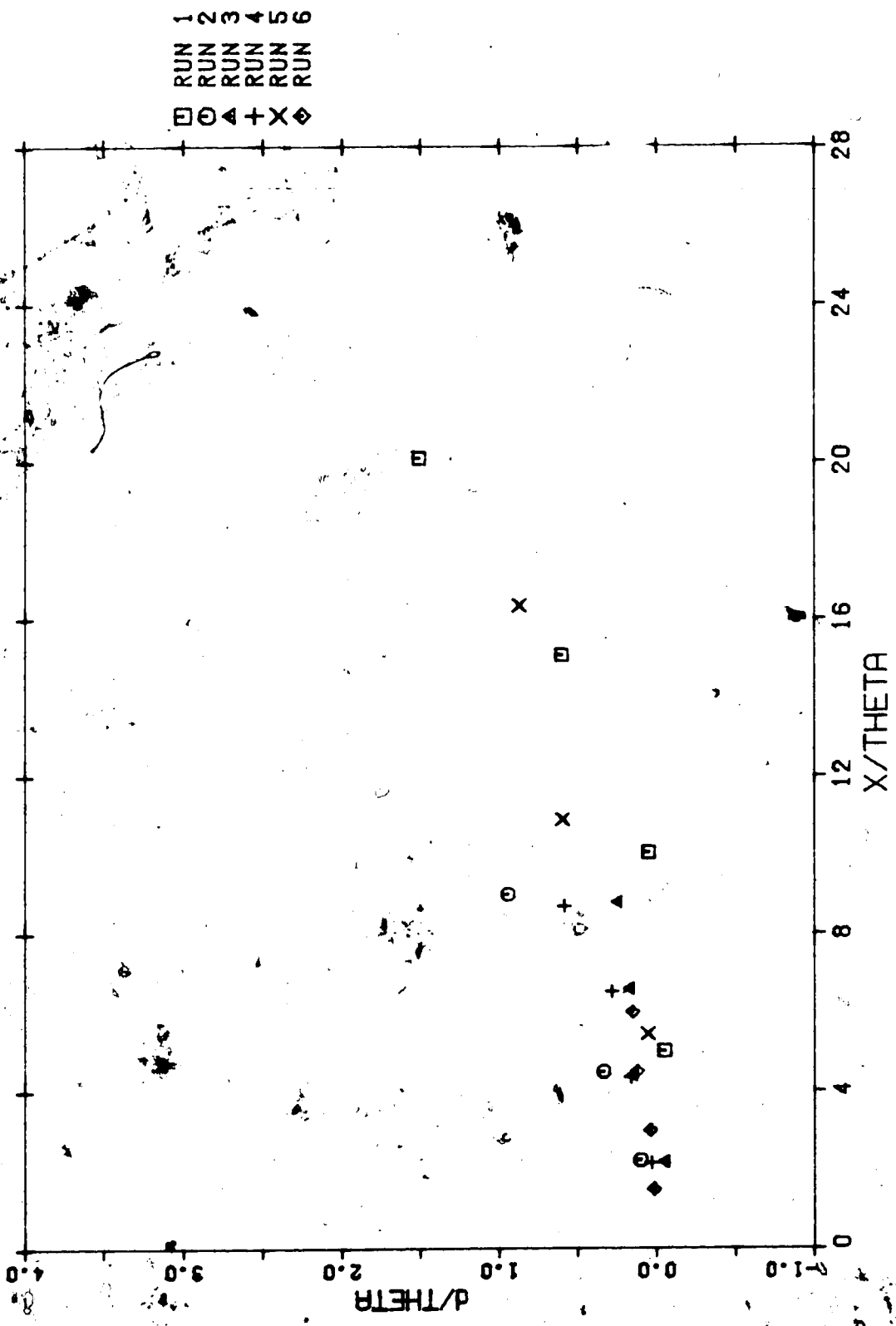
Figure 37 - Prediction of Jet Deflection - Circular Wall
Jets in Curved Channel Flow

2. THEORETICAL INVESTIGATION

2.1 Theoretical Analysis

2.1.1 Preliminary Remarks

The exper.   al work above showed that the jet
parameters and similarity profiles were not significantly
altered by the presence of the crossflow. The jet, however,
was deflected to follow a curved path. In this chapter a
theoretical analysis based on an assumption of a weak
crossflow will be presented.

To start with, for simplicity, the case of a plane.
turbulent jet in a uniform crossflow will be studied. The
technique developed will then be applied to the more
complicated problems of a circular compound jet as well as
to the circular wall jet in a curved stream.

2.1.2 Plane Jet in Uniform Crossflow

Refering to figure (38), the definition sketch for a
plane jet in a crossflow. the situation is that of a plane
jet of initial velocity U_0 and width $2b_0$ issuing into an
ambient fluid with a velocity V in a direction perpendicular
to the jet axis. The parameters which characterize the
velocity field are: the maximum 'x' component of velocity at
any section, u_m, the half velocity width of the jet b , and
the deflection of the jet, d, defined to be the distance
from the outlet axis to the location of velocity maximum.
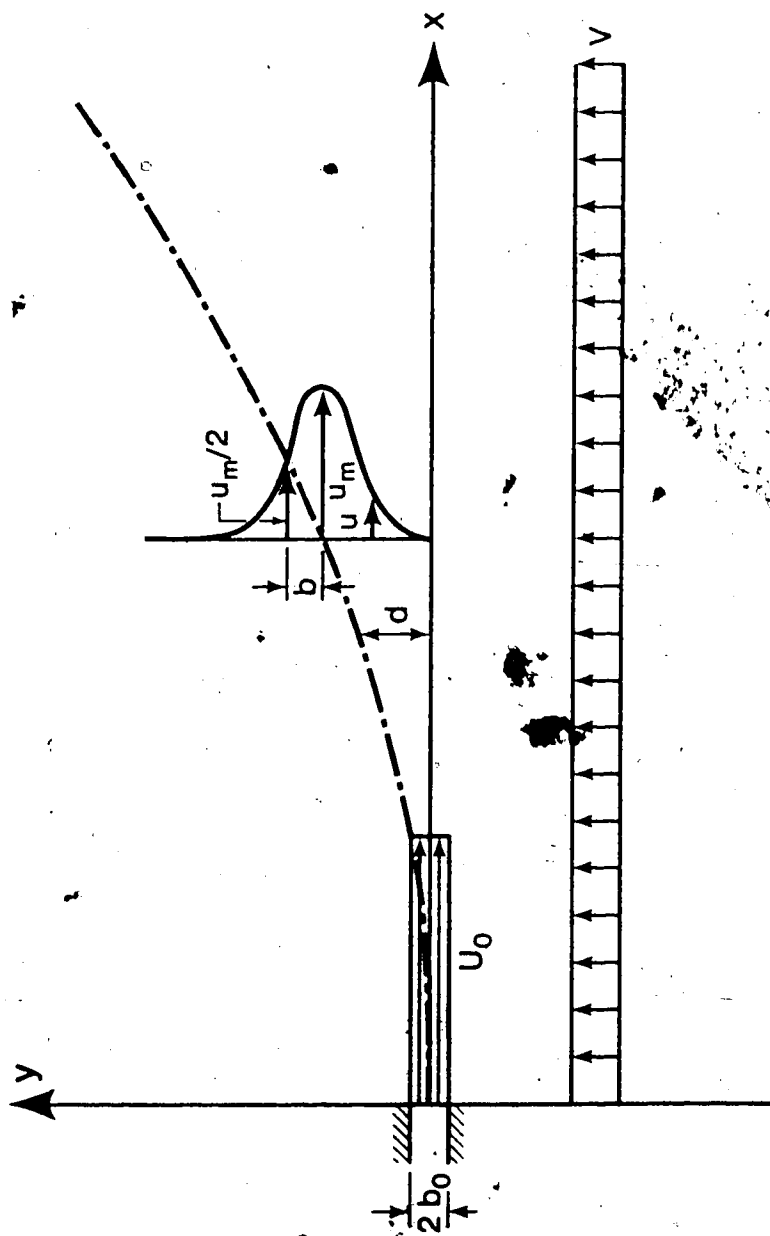
Figure 38. Definition Sketch of Plane Jet in Crossflow.

Assuming V is of the order of magnitude of v′ and the pressure gradient terms are negligable, the equations of motion for this problem reduce to (see the appendix for reduction):

$$u\frac{\partial u}{\partial x} + v'\frac{\partial u}{\partial y} + V\frac{\partial u}{\partial y} = \frac{1}{\rho}\frac{\partial \tau}{\partial y} \tag{5}$$

$$\frac{\partial u}{\partial x} + \frac{\partial v'}{\partial y} = 0 \tag{6}$$

Where:

$$v' = v - V \tag{7}$$

The prime on v′ will be dropped from this point on for convienience. Integral relationships will now be developed to predict u_m, b , and d.

2.1.2.1 Integral Momentum Equation

Integrate equation (5) with respect to y from minus infinity to plus infinity to obtain:

$$\int_{-\infty}^{\infty} \frac{\partial u^2}{\partial x}dy + \int_{-\infty}^{\infty} \frac{\partial uv}{\partial y}dy + \int_{-\infty}^{\infty} \frac{\partial uV}{\partial y}dy = \int_{-\infty}^{\infty} \frac{1}{\rho}\frac{\partial \tau}{\partial y}dy \tag{8}$$

since u and τ equal zero at plus and minus infinity, this
equation reduces to:

$$\frac{d}{dx} \int_{-\infty}^{\infty} u^2 \ dy = 0 \tag{9}$$

This equation states that total axial momentum flux is
conserved.

2.1.2.2 Integral Energy Equation

Multiply equation (5) through by u and use (6) to
rearrange it into:

$$\frac{\partial u^3}{\partial x} + \frac{\partial u^2 v}{\partial y} + \frac{\partial u^2 V}{\partial y} = \frac{2}{\rho} \ u \ \frac{\partial \tau}{\partial y} \tag{10}$$

Again, integrate with respect to y as before.

$$\int_{-\infty}^{\infty} \frac{\partial u^3}{\partial x} dy + \int_{-\infty}^{\infty} \frac{\partial u^2 v}{\partial y} dy + \int_{-\infty}^{\infty} \frac{\partial u^2 V}{\partial y} dy = \frac{2}{\rho} \int_{-\infty}^{\infty} u \ \frac{\partial \tau}{\partial y} \tag{11}$$

Simplifying, the integral energy equation is obtained.

$$\frac{d}{dx} \int_{-\infty}^{\infty} u^3 dy = \frac{2}{\rho} \int_{-\infty}^{\infty} u \ \frac{\partial \tau}{\partial y} \ dy \tag{12}$$

This equation states that the rate of change of total

kinetic energy flux in the jet is equal to the dissipation caused by the shear stress.

2.1.2.3 Comment

The transverse velocity V has disappeared from both the momentum and energy equations which would seem to imply that it has no effect on the axial momentum and energy balances.

2.1.2.4 Integral Moment of Momentum Equation

Multiply equation (5) through by y and integrate as above:

$$\int_{-\infty}^{\infty} \frac{\partial y u^2}{\partial x} dy + \int_{-\infty}^{\infty} y \frac{\partial uv}{\partial y} dy + \int_{-\infty}^{\infty} y \frac{\partial uV}{\partial y} dy = \frac{1}{\rho} \int_{-\infty}^{\infty} y \frac{\partial \tau}{\partial y} dy \tag{13}$$

Integrating the second, third, and fourth terms by parts:

$$\frac{d}{dx} \int_{-\infty}^{\infty} y\, u^2\, dy - \int_{-\infty}^{\infty} u\, v\, dy - \int_{-\infty}^{\infty} u\, V\, dy = -\frac{1}{\rho} \int_{-\infty}^{\infty} \tau\, dy \tag{14}$$

Since u goes to zero exponentially the terms evaluated at infinity are all equal to zero. The remaining term involving shear stress is also zero by antisymmetry. This leaves:

$$\frac{d}{dx} \int_{-\infty}^{\infty} y\, u^2 dy - \int_{-\infty}^{\infty} u\, v\, dy - \int_{-\infty}^{\infty} u\, V\, dy = 0 \tag{15}$$

Consider the second and third terms. It may be noted that in the second term v will be small where u is largest and also that v will tend to have opposite signs on opposite sides of the jet. Thus the integral will tend to be small. If V is of the same order of magnitude as v then the third term will clearly be much larger and the second may be neglected. (Note: In an undeflected jet v is antisymmetric and u is symmetric resulting in the integral going to zero identically. In the weakly deflected case considered here u remains symmetric but v is no longer antisymmetric. The deviation, however, is small.) Thus the following is obtained.

$$\frac{d}{dx} \int_{-\infty}^{\infty} y \, u^2 dy = \int_{-\infty}^{\infty} u \, V \, dy \tag{16}$$

This equation may be interpreted as stating that the rate of change of the total flux of moment of momentum equals the convection of $\bar{u}$ velocity in the y direction.

2.1.2.5 Similarity Hypothesis

Following the experimental analysis and preliminary remarks the profile of u velocity in the y direction is assumed to be similar, or:

$$\frac{u}{u_m} = f_1\left(\frac{y - d}{b}\right) = f_1(\eta) \tag{17}$$

Also assume:

$$\frac{\tau}{\rho\, u_m^2} = f_2\left(\frac{y-d}{b}\right) = f_2(\eta) \qquad (18)$$

Note that:

$$y = \eta b + d \qquad (19)$$

$$dy = b\, d\eta \qquad (20)$$

Substitute equations (17), (18), (19), and (20) into equations (9), (12), and (16) to obtain:

$$\frac{d}{dx} u_m^2 b \int_{-\infty}^{\infty} f_1^2 d\eta = 0 \qquad (21)$$

$$\frac{d}{dx} u_m^3 b \int_{-\infty}^{\infty} f_1^3 d\eta = 2\, u_m^3 \int_{-\infty}^{\infty} f_1\, f_2' d\eta \qquad (22)$$

$$\frac{d}{dx} \int_{-\infty}^{\infty} (\eta \; b + d) \; u_m^2 f_1^2 b \; d\eta = \int_{-\infty}^{\infty} V \; u_m \; f \; b \; d\eta \qquad (23)$$

Simplify to get:

$$\frac{d}{dx} (u_m^2 b) = 0 \qquad (24)$$

$$\frac{d}{dx} u_m^3 b \int_{-\infty}^{\infty} f_1^3 d\eta = 2 \; u_m^3 \int_{-\infty}^{\infty} f_1 \; f_2' d\eta \qquad (25)$$

$$\frac{d}{dx} (u_m^2 b \; d) = \frac{I_1}{I_2} V \; b \; u_m \qquad (26)$$

It may be noted that equations (24) and (25) are identical to the corresponding equations for an undeflected jet. Since these equations do not contain d or V they may be solved to give u_m and b . The solution will be identical to the case of an undeflected jet except for a possible difference in the empirical constant. Assuming for now that the constants will indeed be the same, Rajaratnam(1976) gives the solutions as:

$$\frac{u_m}{U_0} = \frac{3.50 \; \nu}{\sqrt{x / \textbf{b}}} \qquad (27)$$

$$b = 0.097 \; x \qquad (28)$$

These expressions may now be substituted into (26) to calculate d. Letting:

$$I_1 = \int_{-\infty}^{\infty} f_1 \; d\eta \qquad (29)$$

$$I_2 = \int_{-\infty}^{\infty} f_1{}^2 d\eta \qquad (30)$$

and substituting (27) and (28) into (26):

$$\frac{d}{dx} \frac{(3.5 \; U_0)^2 \; b_0 \; (0.097 \; x) \; d}{x} = \frac{I_1}{I_2} \; U_0 \; V \; (0.097 \; x) \left[\frac{3.50}{\sqrt{x \; / \; b_0}} \right] \qquad (31)$$

Rearranging:

$$\frac{dd}{dx} = 0.286 \; \frac{I_1}{I_2} \; \frac{V}{U_0} \sqrt{\frac{x}{b_0}} \qquad (32)$$

Solving the differential equation with the initial condition:

$$d = 0 \quad \text{at} \quad x = 0 \tag{33}$$

we obtain:

$$\frac{d}{b_0} = 0.19 \frac{V}{U_0} \frac{I_1}{I_2} \left(\frac{x}{b_0}\right)^{3/2} \tag{34}$$

Evaluating constants using the convienient exponential form for f:

$$f(\eta) = e^{-0.693 \eta^2} \tag{35}$$

gives:

$$I_1 = 1.063 \tag{36}$$

$$I_2 = 0.751 \tag{37}$$

Finally, substituting for these constants we obtain:

$$\frac{d}{b_0} = 0.27 \frac{V}{U_0} \left(\frac{x}{b_0}\right)^{3/2} \tag{38}$$

Equation (38) gives the deflection of a simple plane jet as a function of downsteam distance and initial jet parameters.

2.1.3 Circular Compound Jet In Uniform Crossflow

The technique for analysing a circular compound jet in a uniform crossfow is identical to that used to analyse the plane jet. The symmetry conditions, however, are no longer satisfied and it will be necessary to integrate in both cross-sectional directions. The more complicated boundary conditions at infinity will also result in added complexity in both the analysis and final expression for the deflection. Refering to the definition sketch, figure (39), the additional parameters are the background axial velocity U and b is now the nozzle diameter. The equations of motion for this problem are:

$$\frac{\partial u}{\partial x} + \frac{\partial v}{\partial y} + \frac{\partial w}{\partial z} = 0 \tag{39}$$

$$u\frac{\partial u}{\partial x} + v\frac{\partial u}{\partial y} + w\frac{\partial u}{\partial z} + U\frac{\partial u}{\partial x} + V\frac{\partial u}{\partial y} = \frac{1}{\rho}\left(\frac{\partial \tau_{xy}}{\partial y} + \frac{\partial \tau_{zx}}{\partial z}\right) \tag{40}$$
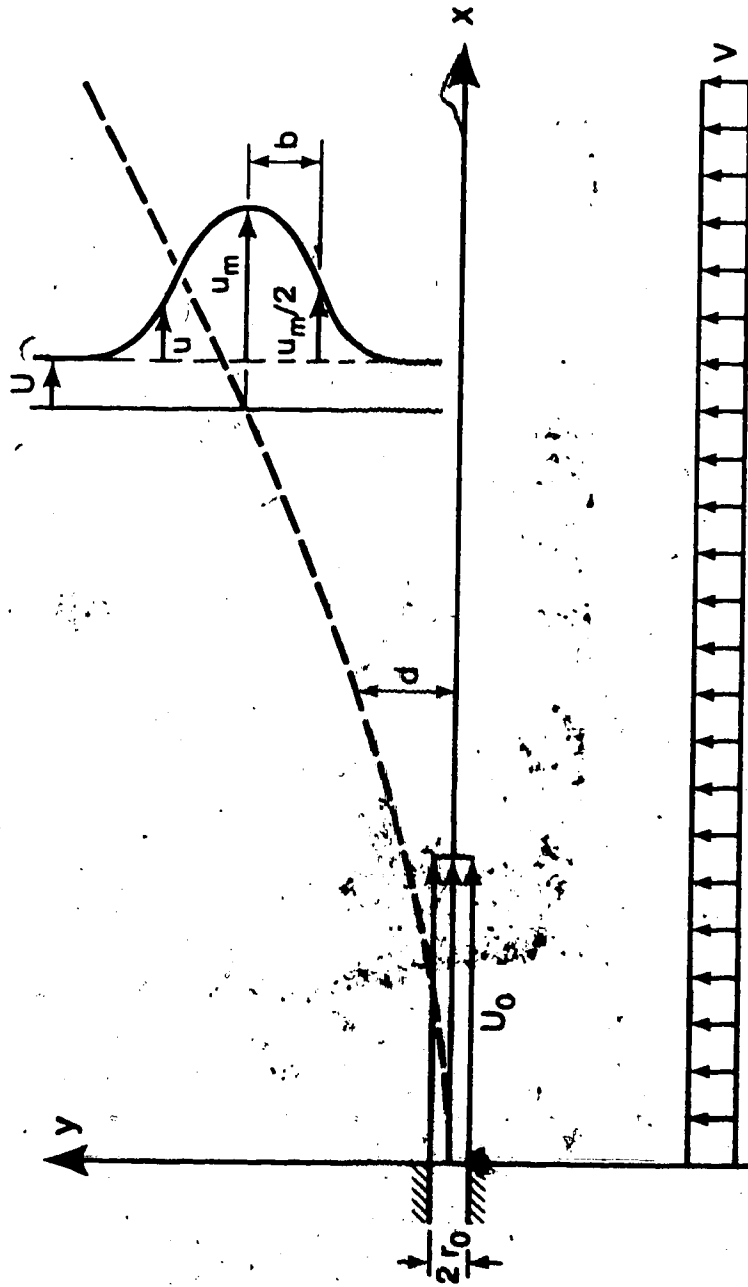
Figure 39. Definition Sketch of Circular Compound Jet in Crossflow.

2.1.3.1 Integral Momentum Equation

Integrate (40) with respect to 'z' from minus to plus infinity.

$$\frac{\partial}{\partial x}\int_{-\infty}^{\infty} u^2 dz + \int_{-\infty}^{\infty}\frac{\partial uv}{\partial y}dz + \frac{\partial}{\partial x}\int_{-\infty}^{\infty} U\,u\,dz + \int_{-\infty}^{\infty}\frac{\partial \tau_{zx}}{\partial y}\,dz = \frac{1}{\rho}\int_{-\infty}^{\infty}\frac{\partial \tau_{yx}}{\partial y}\,dz \qquad (42)$$

Now integrate (42) with respect to 'y' from minus infinity to plus infinity and simplify as above.

$$\frac{d}{dx}\int\int_{-\infty}^{\infty} u\,(U + u)\,dy\,dz = 0 \qquad (43)$$

This equation, the integral momentum equation, states that the exess momentum efflux of the jet is conserved.

2.1.3.2 Integral Energy Equation

Multiply equation (40) by 'u' and use (39) to obtain:

$$\frac{\partial u^3}{\partial x} + \frac{\partial u^2 v}{\partial y} + \frac{\partial u^2 w}{\partial z} + \frac{\partial U\,u^2}{\partial x} + \frac{\partial V\,u^2}{\partial y} = \frac{2u}{\rho}\left(\frac{\partial \tau_{xy}}{\partial y} + \frac{\partial \tau_{zx}}{\partial z}\right) \qquad (44)$$

Integrating with respect to 'z' and 'y' as above and simplifying the integral energy equation is obtained.

$$\frac{d}{dx}\int\int_{-\infty}^{\infty} u^2(U + u)\,dy\,dz = \int\int_{-\infty}^{\infty}\frac{2u}{\rho}\left(\frac{\partial \tau_{yx}}{\partial y} + \frac{\partial \tau_{zx}}{\partial z}\right)\,dy\,dz \qquad (45)$$

This equation states that the rate of change of total energy efflux equals the dissipation by shear, stresses.

Note once again that the crossflow V does not appear in the equations. If we assume that the width scales are the same in both cross-sectional directions, then these two equations can be solved for u_m and b. Note also that these equations are the same as the equations derived by Pande and Rajaratnam (1979) (though in a different form).

2.1.3.3 Integral Moment of Momentum Equation

Multiply equation (40) by 'y' and integrate with respect to 'z' from minus infinity to plus infinity.

$$\int_{-\infty}^{\infty} \frac{\partial yu^2}{\partial x} dz + \int_{-\infty}^{\infty} y \frac{\partial uv}{\partial y} dz + \int_{-\infty}^{\infty} \frac{\partial U y u}{\partial x} dz + \int_{-\infty}^{\infty} y \frac{\partial Vu}{\partial y} dz = \int_{-\infty}^{\infty} y \frac{\partial \tau_{yx}}{\partial y} dz. \quad (46)$$

Integrate again with respect to 'y' from minus infinity to plus infinity.

$$\frac{d}{dx} \iint_{-\infty}^{\infty} yu (u + U) \, dy \, dz + \iint_{-\infty}^{\infty} y \frac{\partial uv}{\partial y} dy \, dz + \iint_{-\infty}^{\infty} y \frac{\partial Vu}{\partial y} dy \, dz$$

$$= \frac{1}{\rho} \iint_{-\infty}^{\infty} y \frac{\partial \tau_{yx}}{y} dy \, dz \quad (47)$$

Integrating the second term by parts:

$$\int_{-\infty}^{\infty} y \frac{\partial uv}{\partial y} dy = [y \, u \cdot v]_{-\infty}^{\infty} - \int_{-\infty}^{\infty} u \, v \, dy \quad (48)$$

Similarily the third term:

$$\int_{-\infty}^{\infty} y \frac{\partial Vu}{\partial y} dy = \left[y\ V\ u \right]_{-\infty}^{\infty} - \int_{-\infty}^{\infty} u\ V\ dy \tag{49}$$

And the fourth term.

$$\int_{-\infty}^{\infty} y \frac{\partial \tau_{xy}}{\partial y} dy = \left[y\ \tau_{yz} \right]_{-\infty}^{\infty} - \int_{-\infty}^{\infty} \tau_{yx}\ dy \tag{50}$$

Collecting the remaining terms:

$$\frac{d}{dx} \iint_{-\infty}^{\infty} y\ u\ (U + u)\ dy\ dz - \iint_{-\infty}^{\infty} u\ V\ dy\ dz - \iint_{-\infty}^{\infty} u\ V\ dy\ dz \tag{51}$$

$$= \frac{-1}{\rho} \iint_{-\infty}^{\infty} \tau_{yx}\ dy\ dz$$

The last term may be set equal to zero by antisymmetry. As in the plane jet, the second term, while not identically zero, is small compared to the third term and may be neglected. Finally:

$$\frac{d}{dx} \iint_{-\infty}^{\infty} y\ u\ (U + u)\ dy\ dz = \iint_{-\infty}^{\infty} u\ V\ dy\ dz \tag{52}$$

2.1.3.4 Similarity Hypothesis

Assume:

$$\frac{u}{u_m} = f_1\left(\frac{z}{b}\right) g_1\left(\frac{y-d}{b}\right) = f_1(\zeta) \, g_1(\eta) \tag{53}$$

where f1 and g1 are the similarity profiles in the z and y directions. Note that the width scale b is assumed to be the same in both directions. Also assume:

$$\frac{\tau_{yx}}{\rho \, u_m^2} = f_2(\zeta) \, g_2(\eta) \tag{54}$$

$$\frac{\tau_{zx}}{\rho \, u_m^2} = f_3(\zeta) \, g_3(\eta) \tag{55}$$

Now substitute these similarity expressions into equations (43), (45) and (52).

$$\frac{d}{dx} \iint_{-\infty}^{\infty} u_m \, b^2 \, f_1 g_1 \left(1 + \frac{u_m}{U} f_1 g_1\right) d\eta \, d\zeta = 0 \tag{56}$$

$$\frac{d}{dx}\left[u_m^2 b^2 \iint_{-\infty}^{\infty} f_1^2 g_1^2 \left(1 + \frac{u_m}{U} f_1 g_1\right) d\eta \, d\zeta\right] \tag{57}$$

$$= 2 \frac{u_m^3}{b \, U} \iint_{-\infty}^{\infty} f_1 \, g_1 \, (f_2 \, g_2' + f_3 \, g_3) \, d\eta \, d\zeta$$

$$\frac{d}{dx} u_m b^2 \iint\limits_{-\infty}^{\infty} f_1 \ g_1 \ d \ (U + u_m \ f_1 \ g_1) \ d\eta \ d\zeta = V \ u_m \ b^2 \iint\limits_{-\infty}^{\infty} f_1 \ g_1 \ d\eta \ d\zeta \qquad (58)$$

Equations (56) and (57) are found to be identical to the corresponding equations for an undeflected jet. The parameters u_m and b are therefore given by the analysis of Pande and Rajaratnam(1979), as:

$$\frac{U}{u_m} \simeq \frac{1}{K} \left(\frac{x}{\theta}\right) \quad \text{for} \quad \frac{x}{\theta} < 150 \qquad (59)$$

$$b = \frac{1}{2} \frac{\theta^2}{\left(\frac{u_m}{U}\right)^2 F_2 + \left(\frac{u_m}{U}\right) F_1} \qquad (60)$$

where

$$\theta = r_c \sqrt{\frac{u_0}{U} \cdot \left(\frac{u_0}{U} - 1\right)} \qquad (61)$$

is the momentum thickness and K is a constant taken to be equal to 12.17. Rewriting equation (58)

$$\frac{d}{dx} \left(u_m \ b^2 d \ (U_1 \ I_4 + u_m \ I_5)\right) = V \ u_m \ b^2 \ I_4 \qquad (62)$$

where

$$I_4 = \iint\limits_{-\infty}^{\infty} f_1 \, g_1 \, d\eta \, d\zeta \tag{63}$$

$$I_5 = \iint\limits_{-\infty}^{\infty} f_1{}^2 g_1{}^2 d\eta \, d\zeta. \tag{64}$$

Substituting (59), (60), (63) and (64) into (62):

$$\frac{d}{dx}\left\{ \frac{x}{F_2 + (x/\theta) F_1} \left[I_4 + \frac{K I_5}{(x/\theta)} \right] \right\} = \frac{V}{U} \frac{I_4 (x/\theta)}{(K F_2 + (x/\theta)F_1)} \tag{65}$$

Expand derivative:

$$\frac{dd}{dx} + \frac{d}{\theta} \frac{K (F_2 I_4 - F_1 I_5)}{(F_1 (x/\theta) + K F_2)(I_4 (x/\theta) + K I_5)} = \frac{V}{U} \frac{I_4 (x/\theta)}{K I_5 + I_4 (x/\theta)} \tag{66}$$

Using equation (4) for both f1 and g1 we may evaluate the constants as:

$$I_4 = \iint\limits_{-\infty}^{\infty} e^{-0.693(\eta^2 + \zeta^2)} \, d\eta \, d\zeta = 4.533 \tag{67}$$

$$I_5 = \iint\limits_{-\infty}^{\infty} e^{-0.693(2)(\eta^2 + \zeta^2)} \, d\eta \, d\zeta = 2.266 \tag{68}$$

From Pande and Rajaratnam (1979)

$$F_1 = 0.7215 \tag{69}$$

$$F_2 = 0.3608 \tag{70}$$

therefore:

$$(F_2 I_4 - F_1 I_5) = 0 \tag{71}$$

Thus we obtain the simplified form:

$$\frac{dd}{dx} = \frac{V}{U} \frac{(x/\theta)}{((x/\theta) + (K/2))} \tag{72}$$

This may be easily integrated to give:

$$\frac{d}{\theta} = \frac{V}{U} \left\{ \frac{x}{\theta} - \frac{K}{2} \ln\left[\frac{(x/\theta) + (K/2)}{(K/2)} \right] \right\} \tag{73}$$

Again, we have a simple expression for the calculation of jet deflection.

2.1.3.5 Simple Jet As a Special Case

Take equation (72) again:

$$\frac{dd}{dx} = \frac{V}{U} \frac{(x/\theta)}{((x/\theta) + (K/2))} \tag{74}$$

Since:

$$\theta = r_0 \sqrt{\frac{U_0}{U} \left[\frac{U_0}{U} - 1\right]} \tag{75}$$

We have:

$$\frac{dd}{dx} = \frac{1}{r_0 \, U \sqrt{\frac{U_0}{U} \left[\frac{U_0}{U} - 1\right]}} \frac{V \, x}{\left(\frac{x}{r_0} \frac{1}{\sqrt{\frac{U_0}{U} \left[\frac{U_0}{U} - 1\right]}} + \frac{K}{2}\right)} \tag{76}$$

Setting U equal to zero:

$$\frac{dd}{dx} = \frac{2 \, V \, x}{K \, r_0 \, U_0} \tag{77}$$

Solving:

$$\frac{d}{r_0} = \frac{1}{K} \frac{V}{U_0} \left(\frac{x}{r_0}\right)^2 \tag{78}$$

2.1.4 <u>Jet</u> <u>Discharging</u> <u>On</u> <u>Bed</u> <u>Of</u> <u>Curved</u> <u>Channel</u>

The theory developed above will now be applied to predict the jet deflection in a complicated practical situation. The problem will be idealized as a three dimensional compound wall jet with a linearly varying crossflow. In this case no analytical solution exists that the writer is aware of for the undeflected case. However, the experimental results of both the present study and that of Stalker(1979) may be used instead to provide the necessary information about the variation of width and velocity scales. Therefore, only the integral moment of momentum equation will be derived and used.

2.1.4.1 <u>Integral</u> <u>Moment</u> <u>of</u> <u>Momentum</u> <u>Equation</u>

Multiplying equation (40) by 'y' and integrating with respect to 'z' from z = 0 to z = ∞ we obtain:

$$\int_0^\infty \frac{\partial y u^2}{\partial x}\, dz + \int_0^\infty \frac{\partial uv}{\partial y}\, dz + \int_0^\infty \frac{\partial Uuy}{\partial x}\, dz + \int_0^\infty y\, \frac{\partial Vu}{\partial y}\, dz$$

$$= \frac{1}{\rho}\int_0^\infty y\, \frac{\partial \tau_{yx}}{\partial y}\, dz - \frac{1}{\rho}\, y\, \tau_{zx} \tag{79}$$

Integrate now with respect to y from y = -∞ to y = ∞ :

$$\frac{d}{dx}\int_{-\infty}^\infty\int_0^\infty y\, u^2 dy\, dz + \int_{-\infty}^\infty\int_0^\infty y\, \frac{\partial uv}{\partial y}\, dy\, dz + \int_{-\infty}^\infty\int_0^\infty \frac{\partial Uuy}{\partial x}\, dy\, dz + \int_{-\infty}^\infty\int_0^\infty y\, \frac{\partial uV}{\partial y}\, dy\, dz \tag{80}$$

$$= \frac{1}{\rho}\int_{-\infty}^\infty\int_0^\infty y\, \frac{\partial \tau_{yx}}{\partial y}\, dy\, dz - \frac{1}{\rho}\int_{-\infty}^\infty\int_0^\infty y\, \tau_{zx}\, dy$$

Evaluating the terms as above:

$$\frac{d}{dx} \iint_{-\infty}^{\infty}\int_{0}^{\infty} y \, u \, (U + u) \, dy \qquad \iint_{-\infty}^{\infty}\int_{0}^{\infty} u \, V \, dy \, dz = 0 \qquad (81)$$

Thus the integral moment of momentum equation is identical to that of the previous section. In this case however the two length scales may not be taken as equal.

2.1.4.2 Similarity Hypothesis

Substituting the similarity hypothesis into equation (81):

$$\frac{d}{dx} u_m \, b_y \, b_z \iint_{-\infty}^{\infty}\int_{0}^{\infty} f_1 \, g_1 \, d \, (U + u_m \, f_1 \, g_1) \, d\eta \, d\zeta \qquad (82)$$

$$b_z \, b_y \iint_{-\infty}^{\infty}\int_{0}^{\infty} g_1 \, d\eta \, d\zeta$$

or:

$$\frac{d}{dx} \left[u_m \, b_y \, b_z \, d \, (U \, I_6 + u_m \, I_7) \right] = V \, u_m \, b_z \, b_y \, I_6 \qquad (83)$$

where

$$I_6 = \iint_{-\infty}^{\infty}\int_{0}^{\infty} f_1 \, g_1 \, d\eta \, d\zeta \qquad (84)$$

$$I_7 = \iint_{-\infty}^{\infty}\int_{0}^{\infty} f_1^2 f_2^2 d\eta \, d\zeta \qquad (85)$$

To solve for d we will assume:

$$\frac{b_z}{\theta} = K_1 \frac{x}{\theta} \tag{86}$$

$$\frac{b_y}{\theta} = K_2 \frac{x}{\theta} \tag{87}$$

$$\frac{U}{u_m} = K_3 \frac{x}{\theta} + K_4 \left(\frac{x}{\theta}\right) \tag{88}$$

where the K's are to be determined from experiment. Nondimensionalize variables by letting

$$\xi = \frac{x}{\theta}, \quad \delta = \frac{d}{\theta}, \quad \beta = \frac{V}{U} \tag{89}$$

Substitute the above into equation and simplify to obtain:

$$\frac{d}{d\xi}\left[\frac{\delta\ (I_6\ K_4\ \xi^2 + I_6\ K_3\ \xi + I_7)}{(K_3 + K_4\ \xi)^2}\right] = \frac{\beta\ \xi\ I_1}{(K_3 + K_4\ \xi)} \tag{90}$$

Now V is a function of 'x' in this case and is given by:

$$V = V_0 \cos(x/R) + U \sin(x/R) \tag{91}$$

Since x is much smaller than R, this may be approximated as:

$$V = V_0 + U \, (x/R) \tag{92}$$

Substitute into equation (90):

$$\frac{d}{d\xi}\left(\frac{\delta \, (I_6 \, K_4 \, \xi^2 + I_6 \, K_3 \, \xi + I_7)}{(K_3 + K_4 \, \xi)^2}\right) = \frac{I_6 \, \xi \, ((V_0/U) + (\theta/R) \, \xi)}{(K_3 + K_4 \, \xi)} \tag{93}$$

Perform the integration

$$\delta = \frac{I_6 \, (K_3 + K_4 \, \xi)^2}{K_4(I_6 \, K_4 \, \xi^2 + I_6 \, K_3 \, \xi + I_7)}\left[\frac{V_0}{U}\left(\xi - \frac{K_3}{K_4}\ell n\Xi\right)\right.$$

$$\left. + \frac{\theta}{R}\left(\frac{\xi^2}{2} - \frac{\xi \, K_3}{K_4}\ell n\Xi + \frac{K_3^2}{K_4^2}(\Xi \, \ell n\Xi - \Xi + 1)\right)\right] + C \tag{94}$$

Where:

$$\Xi = \left(\frac{K_4}{K_3}\xi + 1\right) \tag{95}$$

Evaluate the constant:

$$\text{at } \xi = 0 \, , \quad \delta = 0 \Rightarrow C = 0 \tag{96}$$

Finally:

$$\delta = \frac{I_6 (K_3 + K_4 \xi)^2}{(I_6 K_4 \xi^2 + I_6 K_3 \xi + I_7)}\left[\frac{V_0}{U}\left(\xi - \frac{K_3}{K_4}\ell n\Xi\right)\right.$$

$$\left. + \frac{\theta}{R}\left(\frac{\xi}{2} - \frac{\xi K_3}{K_4}\ell n\Xi + \frac{K_3^2}{K_4^2}(\Xi \ell n\Xi - \Xi + 1)\right)\right] \tag{97}$$

To evaluate the constants take as a first approximation the similarity profile:

$$f_1 = g_1 = e^{-0.693\eta^2} \tag{98}$$

Thus

$$I_6 = 2.266 \tag{99}$$

$$I_7 = 1.133 \tag{100}$$

Now from the experimental results

$$K_3 = 0.0822 \tag{101}$$

$$K_a = 0.00439 \qquad (102)$$

2.2 Comparison of Theory to Experiment

There is much experimental data concerning the deflection of jets by crossflows. However, there is little data on the particular region or type of jet that was analysed above. At present the data consists of a very few runs at high velocity ratios and perhaps one or two initial points from low velocity ratio runs. Data on compound jets and wall jets is even scarcer.

Figure (40) shows a comparison of equation (78) to compiled data of Pratte and Baines (1967). The agreement is good up to a value of r

$$\frac{V}{U}\frac{x}{b_0} < 1 \qquad (103)$$

Figure (41) compares the same equation to one profile of Rajaratnam and Gangadrahiah and indicates good agreement up to the same limit as above.

Finally equation (97) may be compared to the experimental data obtained previosly in this study. This plot is displayed on figure (42). The magnitude of V was

83
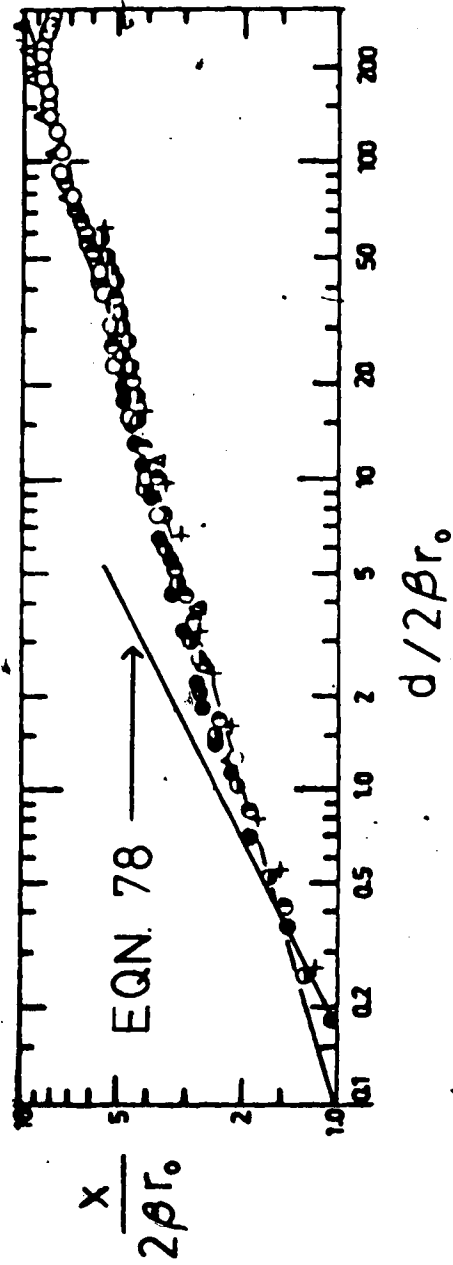
Figure 40 - Comparison of Equation 78 With Pratte and Baines
Deflection Data
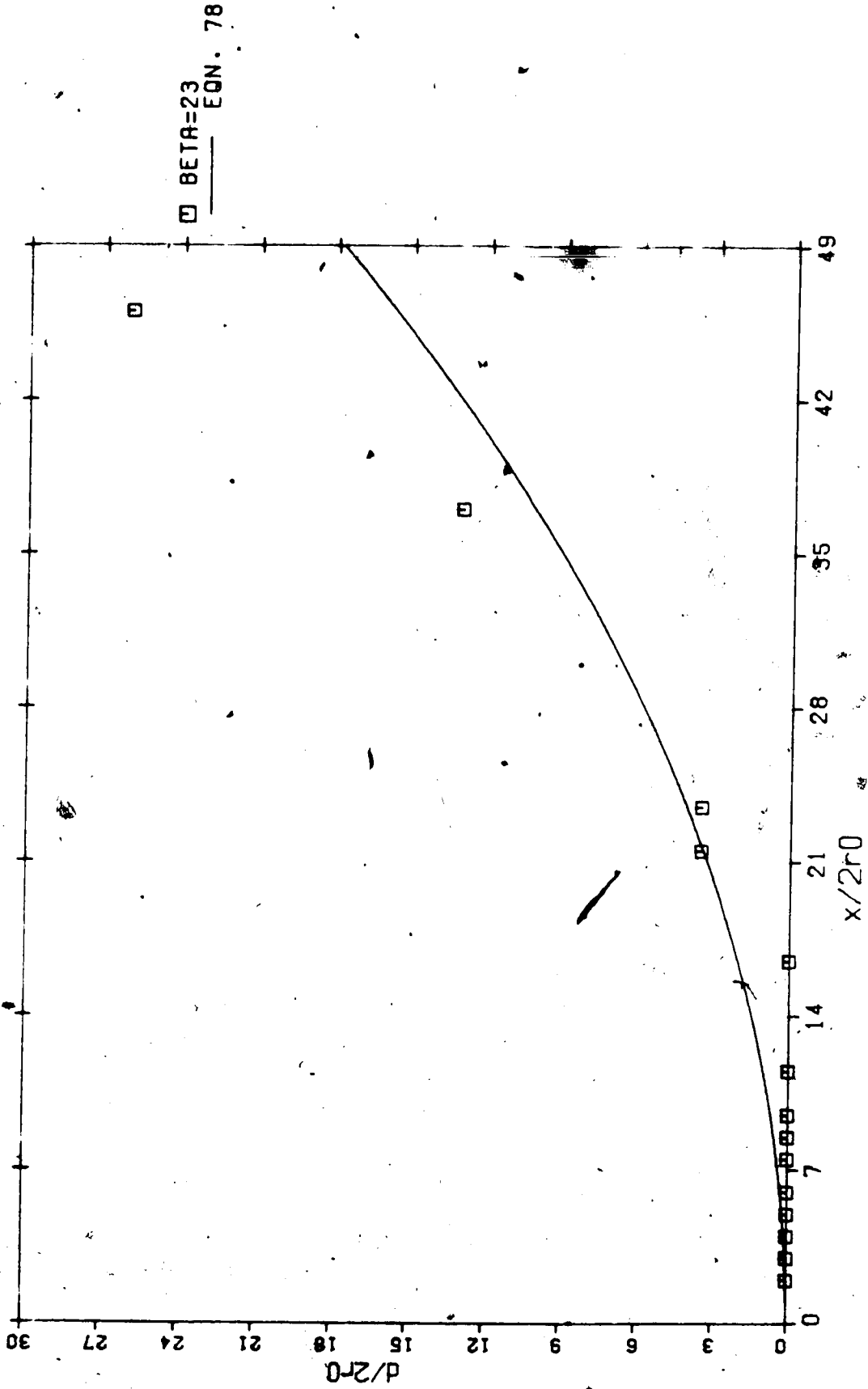
Figure 41 - Comparison of Equation 78 With Rajaratnam and Gangadrahiah Data
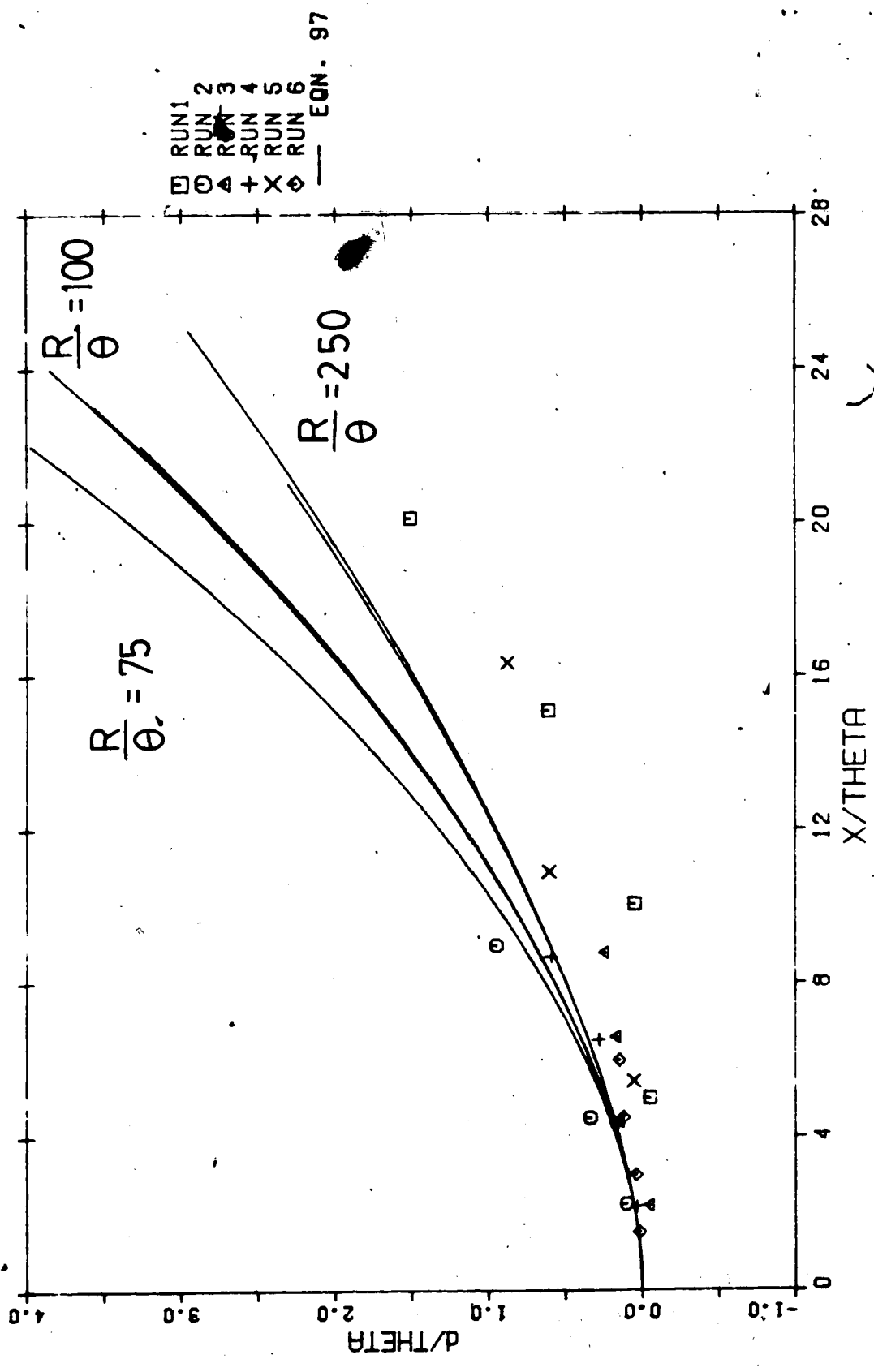
Figure 42 - Prediction of Jet Deflection for Various R/θ and Comparison With Experimental Observations

calculated from equation (3). The theory seems to indicate the magnitude of the deflection fairly well but the large scatter in the data prevents any definate conclusions. The scatter is believed to be caused by difficulty in aligning the jet nozzle with the coordinate system.

2.3 Discussion of Theory

The use of a moment of momentum equation to calculate the deflection is natural since the method is analagous to the calculation of the mean of a statistical distribution. The location of the maximum velocity point is, in fact, the 'mean' location of the jet.

The physical interpretaion of these results may be easily seen by simplification of the final differential equation. Equation (26) for example may be simplified by noting that the corresponding momentum equation reduces to:

$$\frac{d}{dx} (u_m^2 \, b) = 0 \qquad\qquad (104)$$

Thus:

$$\frac{dd}{dx} = \frac{I_1}{I_2} \frac{V}{u_m} \qquad\qquad (105)$$

The deflection is seen to be a consequence of simple

.convection. The constant factor accounts for the non-uniform velocity distribution and thus equation (105) states that the deflection is a consequence of some type of average convection. This equation may be contrasted with equation (2). The essential difference is that the former will apply in cases where the jet characteristics dominate and the latter to cases where they do not.

CONCLUSION

The present work on the deflection of jets by weak crossflows involved an experimental and analytical study. The experimental results provided the qualitative information about similarity and scale variation which allowed the simplification of the analysis. The experiments did not, however, provide a validation for the theory due to a large scatter in the deflections observed. This scatter is believed to have been caused by a crude jet alignment procedure.

The theoretical analysis, involving the use of an integrated moment of momentum equation, provides a simple, direct, method of calculating the deflection of a jet. The method is only valid in the initial region of a weakly deflected jet but there are numerous practical situations where this region is of interest. Advantages of this method are that: it is direct, allowing the use of solutions for undeflected cases; it does not require an empirical constant or function; and it is easily applied in a wide variety of cases.

As suggestions for further study the most important would be accurate and purposeful experimental work on the weakly deflected jet both to provide justification, and the limits thereof, for the theoretical simplifications for a wider variety of situations and to validate the theoretical

calculations. Also of interest would be to attempt to apply
the theory to problems involving bouyancy, both deflection
of a bouyant plume by a crossflow and the deflection of a
jet by a density gradient.

REFERENCES

Abramovich,G. "The Theory of Turbulent Jets" M.I.T. Press,
Massachusetts,1963

Chan, Lin, Kennedy "Entrainment and Drag Forces on Deflected
Jets" ASCE Journal of the Hydraulics Division,
Vol. 102, May , 1976

Crowe, C. and Riesbieter, H. "An Analytical and Experimental
Study of Jet Deflection in a Crossflow" Fluid
Dynamics of Rotor and Fan Supported Aircraft at
Subsonic Speeds, AGARD Preprints, 1967

Engelund, F. "Flow and Bed Topography in Channel Bends" ASCE
Journal of the Hydraulics Division, Vol. 100 ,
November, 1974

Engmann, E. "Transverse Mixing Characteristics of Open and
Ice-covered Channel Flows" Ph.D. Thesis, Dept.
of Civil Engineering, University of Alberta,
1974

Gordier, R. "Studies on Jets Discharging Normally into
         Moving Liquid" St. Anthony Falls Hydraulics Lab.
         , University of Minnesota, Tech Paper 28 ser. B

Keffer, J. and Baines, W. "The Round Turbulent Jet in a
         Crosswind" Journal of Fluid Mechanics, 1963

Makihata and Miyai "Trajectories of Single and Double Jets
         Injected into a Crossflow of Arbitrary Velocity
         Diostribution" ASME Journal of Fluids
         Engineering, Vol 101, June, 1979

Pande, B. and Rajaratnam, N. "Turbulent Jets in Co-Flowing
         Streams" ASCE Journal of the Engineering
         Mechanics Division, Vol. 105, December, 1979

Pani, B. "Three Dimensional Turbulent Wall Jets" PhD Thesis.
         Dept. of Civil Engineering, University of
         Alberta, 1974

Platten, J. and Keffer, J. "Entrainment in Deflected
         Axisymmetric Jets at Various Angles to the

92

Stream" Tech Report 6808, Dept. of Mechanical

Engineering, Univesity of Toronto, 1968

Pratte, B. and Baines, W. "Profiles of the Round Turbulent

Jet in a Crossflow" ASCE Journal of the

Hydraulics Division, Vol 92, 1967

Rajaratnam, N. "Turbulent Jets" Elsevier Scientific

Publishing Co., Amsterdam, 1976

Rozovski, I. "Flow of Water in Bends of Open Channels"

Academy of Sciences of Ukrainian SSR, Kiev,

1957, The Israel Program for Scientific

Translations, 1961

Schlichting, H. "Boundary Layer Theory" McGraw-Hill , New

York, 1979

Stalker, M. "Circular Wall Jets in Co-Flowing Channels" MSc

Thesis, Dept of Civil Engineering, University of

Alberta, 1979

Wright, S. "Mean Behaviour of Bouyant Jets in a Crossflow"
ASCE Journal of the Hydraulics Division, Vol
103, June, 1979

Yen, B. "Characteristics of Subcritical Flow in a Meandering
Channel" Institute of Hydraulic Research,
University of Iowa, Iowa City, 1965

Appendix: Equations of Motion

The equations of motion for a turbulent fluid are (using tensor notation for brevity):

$$\frac{\partial u_i}{\partial t} + u_j \frac{\partial u_i}{\partial x_j} = -\frac{1}{\rho}\frac{\partial p}{\partial x_i} + \frac{1}{\rho}\frac{\partial \tau_{ij}}{\partial x_j} + \frac{\partial \Omega}{\partial x_i} \qquad (A1)$$

$$\frac{\partial u_i}{\partial x_i} = 0 \qquad (A2)$$

where τ_{ij} is composed of a viscous and a turbulent component:

$$\tau_{ij} = -\rho \overline{u_i' u_j'} + \nu \frac{\partial u_i}{\partial x_j} \qquad (A3)$$

It may be shown by order of magnitude analysis that for steady and slender or boundary layer type flows, the above equations reduce to(Pani (1972))

$$u \frac{\partial u}{\partial x} + v \frac{\partial u}{\partial y} + w \frac{\partial u}{\partial z} = \frac{1}{\rho}\frac{\partial p}{\partial x} + \frac{1}{\rho}\frac{\partial \tau_{xy}}{\partial y} + \frac{1}{\rho}\frac{\partial \tau_{xz}}{\partial z} \qquad (A4)$$

$$-\frac{u^2}{r} = -\frac{1}{\rho}\frac{\partial p}{\partial y} + \frac{1}{\rho}\frac{\partial \tau_{yy}}{\partial y} \qquad (A5)$$

$$0 = -\frac{1}{\rho}\frac{\partial p^{\infty}}{\partial z} + \frac{\partial \Omega}{\partial z} \qquad (A6)$$

$$\frac{\partial u}{\partial x} + \frac{\partial v}{\partial y} + \frac{\partial w}{\partial z} = 0 \qquad (A7)$$

where the equations have been written out in a locally cylindrical coordinate system.

This anaysis applies to crossflow situations where V is an order of magnitude smaller than the longitudinal velocity scale and r is of the same order of magnitude as the longitudinal length scale. Equation (A6) is simply the hydrostatic equation and may be discarded for the present purposes.

Integrate equation (A5) with respect to to y from y to infinity to obtain:

$$p_{\infty} - p = \int_{y}^{\infty} \rho\frac{u^2}{r}dy - \tau_{yy} \qquad (A8)$$

Differentiate with respect to x:

$$\frac{\partial p_{\infty}}{\partial x} - \frac{\partial p}{\partial x} = \frac{\partial}{\partial x}\int_{y}^{\infty} \rho\frac{u^2}{r}dy - \frac{\partial \tau_{yy}}{\partial x} \qquad (A9)$$

Thus

$$\frac{1}{\rho}\frac{\partial p}{\partial x} = \frac{1}{\rho}\frac{\partial p_\infty}{\partial x} - \frac{\partial}{\partial x}\int_y^\infty \frac{u^2}{r}dy + \frac{1}{\rho}\frac{\partial \tau_{yy}}{\partial x} \tag{A10}$$

Substitute into equation (A4)

$$u\frac{\partial u}{\partial x} + v\frac{\partial u}{\partial y} + w\frac{\partial u}{\partial z} = -\frac{1}{\rho}\frac{\partial p_\infty}{\partial x} + \frac{\partial}{\partial x}\int_y^\infty \frac{u^2}{r}dy + \frac{1}{\rho}\left(-\frac{\partial \tau_{yy}}{\partial x} + \frac{\partial \tau_{xy}}{\partial y} + \frac{\partial \tau_{xz}}{\partial z}\right) \tag{A11}$$

Applying order of magnitude analysis again, it is found that the fifth and sixth terms are negligable and may be omitted. Further assume that the imposed pressure gradient is negligable.

$$u\frac{\partial u}{\partial x} + v\frac{\partial u}{\partial y} + w\frac{\partial u}{\partial z} = \frac{\partial \tau_{xy}}{\partial y} + \frac{\partial \tau_{xz}}{\partial z} \tag{A12}$$

$$\frac{\partial u}{\partial x} + \frac{\partial v}{\partial y} + \frac{\partial w}{\partial z} = 0 \tag{A13}$$

For the the present purpose it is useful to separate out the ambient flow in these equations so define:

$$v' = v - V \tag{A14}$$

$$u' = u - U \quad . \tag{A15}$$

where U is the ambient co-flowing velocity and V is the ambient crossflow velocity. Noting that V is not a function of y and U is not a function of x equations (A13) and (A14) may be substituted into (A11) and (A12) to give:

$$(u'+ U) \frac{\partial u'}{\partial x} + (v'+ V) \frac{\partial u'}{\partial y} + w \frac{\partial u'}{\partial z} = \frac{\partial \tau_{xy}}{\partial y} + \frac{\partial \tau_{xz}}{\partial z} \tag{A16}$$

$$\frac{\partial u'}{\partial x} + \frac{\partial v'}{\partial y} + \frac{\partial w'}{\partial z} = 0 \tag{A17}$$

These equations and simplifications thereof form the basis of the analytical work in this study. A further conceptual approximation is made in that the these equations are applied in a Cartesian coordinate system whereas they were derived in a locally cylindrical system. Since there are no curvature effects the notation is identical.